Dalton Transactions

Accepted Manuscript

This article can be cited before page numbers have been issued, to do this please use: R. Gil-García, M. Ugalde, N. Busto, H. Lozano, J. M. Leal, B. Pérez, G. Madariaga, M. Insausti, L. Lezama, R. Sanz, L. M. Gómez-Sainz, B. Garcia and J. García-Tojal , *Dalton Trans.*, 2016, DOI: 10.1039/C6DT02907H.

ROYAL SOCIETY OF CHEMISTRY

rsc.li/dalton

View Article Online
DOI: 10.1039/C6DT02907H

Selectivity of a thiosemicarbazonatocopper(II) complex to duplex RNA. Relevant noncovalent interactions both in solid state and in solution

Rubén Gil–García,[a] María Ugalde,[a] Natalia Busto,[a] Héctor J. Lozano,[a] José M. Leal,[a] Begoña Pérez,[a] Gotzon Madariaga,[b] Maite Insausti,[c] Luis Lezama,[c] Roberto Sanz,[a] Lidia M. Gómez-Sainz[a] , Begoña García,*[a] and Javier García–Tojal*[a]

[a] Departamento de Química, Universidad de Burgos, 09001 Burgos, Spain
[b] Departamento de Física de la Materia Condensada, Universidad del País Vasco, Aptdo. 644, 48080 Bilbao, Spain
[c] Departamento de Química Inorgánica, Universidad del País Vasco, Aptdo. 644, 48080 Bilbao, Spain

Keywords: copper, nucleobase, nucleotide, RNA, thiosemicarbazone.

Abstract: Thiosemicarbazones and their metal derivatives have long been screened as antitumor agents and their interactions with DNA have been analyzed. Here, we describe the synthesis and characterization of compounds containing $[CuL]^+$ entities (HL = pyridine-2-carbaldehyde thiosemicarbazone) and adenine, cytosine or 9-methylguanine, and some of their corresponding nucleotides. For the first time, crystal structures of adenine- and 9-methylguanine-containing thiosemicarbazone complexes are reported. To our knowledge, the first research on the affinity thiosemicarbazone-RNA is also provided here. Experimental and computational studies have shown that $[CuL(OH_2)]^+$ entities at low concentration intercalate into dsRNA poly(rA)•poly(rU) through strong hydrogen bonds, involving uracil residues and π–π stacking interactions. In fact, noncovalent interactions are present both in the solid state and in solution. This behaviour diverges from that observed with DNA duplexes and creates an optimistic outlook in achieving selective binding to RNA and its possible medical applications.

Introduction

Ever since the middle of the last century, Brockman et al.[1] began observing anticarcinogenic evidence in the pyridine-2-carbaldehyde thiosemicarbazone molecule (HL, see Scheme 1 with the atom labels used in this work, $R_1 = R_2 = R_3 = H$), the biological properties of thiosemicarbazones have attracted growing attention.[2,3] In particular, those related to their use as antitumour agents have led to clinical trials on HL analogues such as 5-hydroxypyridine-2-carbaldehyde thiosemicarbazone ($R_1 = OH$, $R_2 = R_3 = H$)[4] and 3-aminopyridine-2-carbaldehyde thiosemicarbazone ($R_1 = R_3 = H$, $R_2 = NH_2$, Triapine®), the latter reaching the Phase II stage.[5] Promising preliminary cytotoxic effects against tumour cells have also been detected with metal complexes derived from HL,[6] those with Cu(II) being especially remarkable;[7] actually, the thiosemicarbazone-copper interplay in cells seems to be key to the biological activity of these substances.[8] In particular, Cu(II) ion has aroused special interest due to its rich spectroscopic and magnetic properties that often change in the course of enzyme catalysis.[9] To explain

View Article Online
DOI: 10.1039/C6DT02907H

these interesting features, biochemical studies have revealed that ribonucleotide reductases are usual targets for thiosemicarbazones[10] and, though less studied, other enzymes are also affected.[11] However, thiosemicarbazones can also interact with nucleotide sequences by either intercalation[12] or external binding[13] and, depending on the ligand shape and structure, these compounds can interact with specific polynucleotide sequences.[14] The reaction of DNA with thiosemicarbazonecopper(II) complexes containing heterocyclic ancillary ligands has also been studied. Mechanistic investigations point to either minor or major groove binding, depending on the complex structure.[13,15,16] Unfortunately, the lack of crystallographic support confers uncertainty to the structural features of the interaction.

Previous studies in aqueous solution with $[CuL]^+$ and $[CuL']^+$ entities (HL´ = pyridine-2-carbaldehyde N4-methylthiosemicarbazone, $R_1 = R_2 = H$, $R_3 = CH_3$, see Scheme 1) reveal binding interaction with adenine (Hade), cytosine (Hcyt), guanine (Hgua) and their corresponding nucleoside monophosphates, but not with thymine and thymidine-5'-monophosphate. The most probable linkage proceeds through the nucleobase N sites instead of the phosphate groups, as inferred from the crystal structure of the $[CuL(Hcyt)](ClO_4)$ derivative.[17] The interaction of these thiosemicarbazonatocopper(II) species with $[poly(dA–dT)]_2$, $[poly(dG–dC)]_2$ and ctDNA has also been evaluated, concluding that they undergo groove binding with the DNA A–T tract.[18]

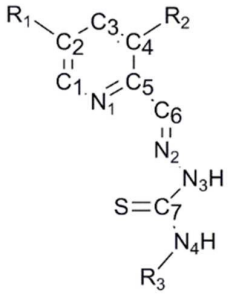

Scheme 1 Atom labels for the thiosemicarbazone ligands.

RNA is involved in a variety of processes in the regulation of the gene expression and can adopt a number of structures and conformations. This polymer displays several cellular functions and provides specific binding sites for small molecules.[19] These conformations offer attractive potential targets for drugs able to bind specifically to such structures, thus enabling the inhibition of the viral transcription.[20]

The molecular requirements for recognition of the duplex RNA have not yet been established. The binding to DNA by organic cation drugs such as Hoechst 33258, berenil or DAPI, exhibit high affinity with the minor groove of A–T tract DNA and intercalate into the RNA duplex. Therefore, the interaction with such molecules creates an optimistic outlook in achieving selective binding of RNA duplex over DNA duplex by tweaking the molecular structure.[21] This binding event requires local opening of the RNA double helix, so the recognition may lie within duplex areas adjacent to bulges or loops, where such opening is available for threading. As we shall see below, a similar behaviour occurs with $[CuL]^+$. To our knowledge, this is the first study on the recognition of duplex RNA by tiosemicarbazones.

To get some insight into the possible binding of thiosemicarbazonatocopper(II) species to DNA, RNA and/or free nucleotide-contained fragments, we present here the crystal structures of compounds in which $[CuL]^+$ entities are linked to Hade, 9-methylguanine (9-Mgua) and Hcyt. Rational synthetic

View Article Online
DOI: 10.1039/C6DT02907H

procedures to get them and some related nucleotides are also discussed (see Scheme 2). Moreover, the interactions of $[CuL]^+$ with 9-Mgua, uracil and poly(rA)□poly(rU) are studied and the biological relevance of the achieved results is evaluated as well. To date, only one work describing crystal studies on the interaction between thiosemicarbazones and nucleobases has been published.[17] Other previous studies have incorporated thiosemicarbazone moieties inside the nucleobase, generating 5-formyluracil thiosemicarbazone ligands.[15, 22] Structural comparison with related Cu(II)-nucleobase systems is discussed to explore the involvement of the noncovalent interactions in the affinity of metal complexes with DNA and RNA.

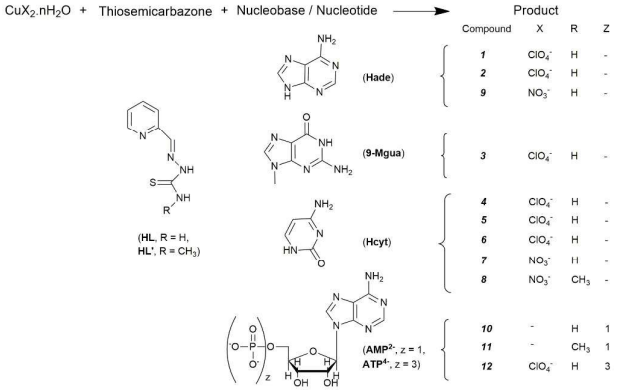

Scheme 2. Summary of the synthesised compounds.

Results and Discussion

Synthesis. Several experiments carried out on the ade⁻/Hade system using water as the only solvent yielded compound ***1*** even at pH 2.0, which confirms the stability of the deprotonated ade⁻ species in the $[\{CuL\}\{CuL(OH_2)\}(ade)]^+$ cation within the pH 2−7 range. Compounds containing both the neutral (Hade) and deprotonated (ade⁻) ligands as ***2***, were isolated as solids with different water content through water/methanol mixtures.

Lack of positive results for the attempts with uracil, thymine and their corresponding nucleotides could be related to the need for sufficient basic aqueous media to ensure deprotonation and further coordination of the nucleobase. In the same way, the low solubility of Hgua in water at physiological pH could prevent from precipitation and isolation of stable ternary complexes. Therefore, we tried to deprotonate the Hgua at pH > 9.0 but, under such reaction conditions, $[CuL]^+$ entities underwent desulfurization that led to formation of $[CuL(L^{CN})]$ [23] [HL^{CN} = pyridine-2-ylmethylene(hydrazinecarbonitrile)] or $[CuLCl]_2[Cu(pic)_2]$ [24] (Hpic = picolinic acid). In fact, partial transformation of $[CuL]^+$ entities into nitrile derivatives in aqueous solutions can be observed even at physiological pH 7.4.[23,24] The conversion in aqueous basic media of sulfur thioamide into sulfate for HL/HL'-Cu(II) species has also been reported.[25] The observed higher solubility in water prompted us to use 9-Mgua instead of Hgua, and then we obtained compound ***3***.

Several trials to attain diverse nucleotide-containing compounds yielded powdered samples for adenosine-5′-monophosphate (H_2AMP) and adenosine-5′-triphosphate (H_4ATP) with large amounts of water, as described below. Attempts using sodium guanosine-5′-monophosphate (Na_2GMP) were

View Article Online
DOI: 10.1039/C6DT02907H

unsuccessful, whereas solids isolated from cytidine-5′-monophosphate (H_2CMP) point to formulae *(CuL)$_2$(HCMP)(ClO$_4$)(H$_2$O)* and *(CuL′)$_2$(HCMP)(ClO$_4$)(H$_2$O)$_4$*, but absence of impurities could not be guaranteed (see Supporting Information). All the efforts for crystallizing the nucleotide derivatives were futile. Thermal decomposition of the nucleobase-containing compounds at 700 ºC yielded CuO (JCPDS No. 72-0629 and 74-1021),[26] while the solid residues in the nucleotide derivatives were a mixture of CuO and some peaks assigned to $Cu_3(PO_4)_2$ (JCPDS No. 80-0991), except for the ATP-containing ***12*** compound, which only showed X-ray peaks of $Cu_2(P_2O_7)$ (JCPDS No. 21-0299, see Figs. S12, S13 and description in Supporting Information).

Crystal structures. Figures 1- 4 depict the drawings with main motifs in the crystal structures of *[{CuL}{CuL(OH$_2$)}(ade)](ClO$_4$)* ***1***, *[(CuL)$_2$(Hade)][{CuL}{CuL(OClO$_3$)}(ade)](ClO$_4$)$_2$·2H$_2$O* ***2***, *[{CuL(9-Mgua)}$_2$(OH$_2$)](ClO$_4$)$_2$* ***3*** and *[CuL(Hcyt)](ClO$_4$)·2H$_2$O* ***4***. Detailed description of the crystal features is given in Supporting Information. All these compounds incorporate anionic tridentate thiosemicarbazones linked to the Cu(II) ions through the $N_{pyridine}$, $N_{azomethine}$ and $S_{thioamide}$ donor atoms, in good agreement with the structural parameters previously reported to distinguish the anion versus neutral forms of the ligand in thiosemicarbazonecopper(II) complexes (see Table S2, Supporting Information).[27]

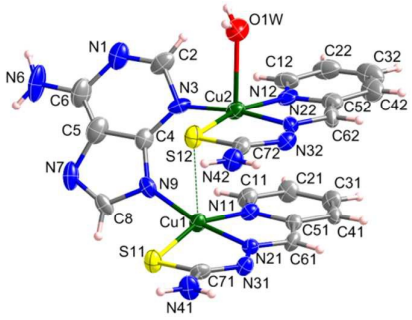

Fig. 1. Crystal structure of the [{CuL}{(CuL)(OH$_2$)}(ade)]$^+$ entity in ***1***. Thermal ellipsoids are drawn at 30% probability level.

Briefly, ***1*** and ***2*** contain dinuclear entities (Figs. 1 and 2, Table S3), where one adenine (μ-κN3: κN9) ligand, neutral or deprotonated after removal of the N7-linked hydrogen atom, acts as a bridge between the Cu(II) ions, retaining the coordinative character usually shown by this nucleobase in non-thiosemicarbazone systems, i.e. on paddle wheel adenine complexes.[28] Another common topic in these compounds is the bridging role of the thioamide sulfur atom, clearer for ***2*** with Cu–S' distances in the 2.80–2.90 Å range, while the length for ***1*** is 3.094(3) Å, regarded as borderline of a real bond despite the place of S12 atom and the Jahn-Teller effect on the Cu(II) ion support the pseudocoordination. Distorted square-planar, elongated octahedral and square-pyramidal[29] topologies around the metal centres are found in these compounds.

View Article Online
DOI: 10.1039/C6DT02907H

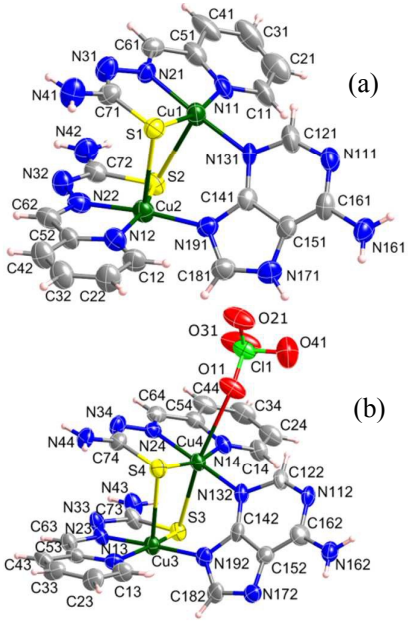

Fig. 2. Crystal structure of the $[(CuL)_2(Hade)]^{2+}$ (a) and $[\{CuL\}\{CuL(OClO_3)\}\{ade\}]$ (b) entities in ***2***. Thermal ellipsoids are drawn at the 20% probability level.

3 is made of dinuclear units where square pyramidal Cu(II) ions present in $[CuL(9\text{-}Mgua)]^+$ fragments are linked by the oxygen atom of a bridging water molecule (Fig. 3, Table S4).

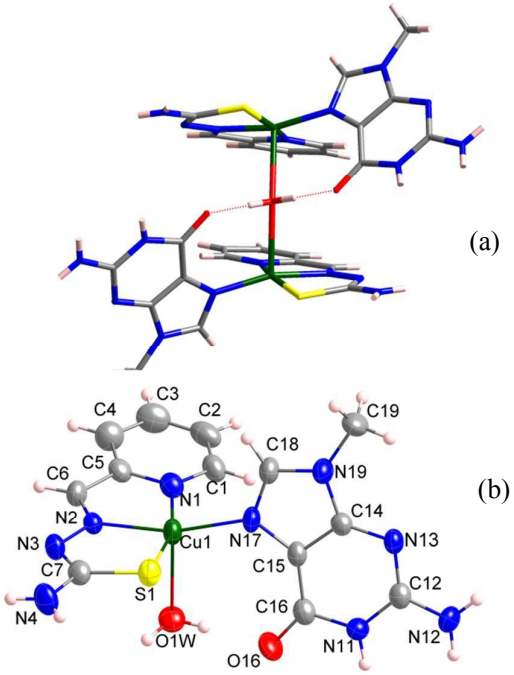

Fig. 3. Crystal structure of $[\{CuL(9\text{-}Mgua)\}_2(OH_2)]^{2+}$ entities (a) and the labelling of its asymmetric unit (b) in *3*. Thermal ellipsoids are drawn at the 50% probability level.

View Article Online
DOI: 10.1039/C6DT02907H

Complex ***4*** is built up by $[CuL(Hcyt)]^+$ monomer units (Fig. 4, Table S4) containing Cu(II) ions with distorted square–planar topology. Notwithstanding, the intramolecular Cu···O12 distance, 2.754(6) Å, could be interpreted as a (4+1) pseudocoordination and falls inside the 2.55–2.88 Å range reported in the literature for the cytosine Cu–O bonds.[30,31] The weakness of such a linkage is suggested by the value of the C12–O12 bond length, 1.246(9) Å, which does not significantly differ from 1.237(2) Å in the free Hcyt.[32] The molecular structure of ***4*** is quite similar to the analogous dehydrated $[CuL(Hcyt)](ClO_4)$ (***5***) compound.[17] A common feature is the formation of π–π stacked dimeric aggregates, which are also stabilized through intra-dimer (N14–H14···N3) hydrogen bonds. However, the entry of water molecules, mainly placed around the cytosine rings (up to seven water molecules closer than 4 Å from cytosine ring), induces differences in the lattice (see Fig. S1).

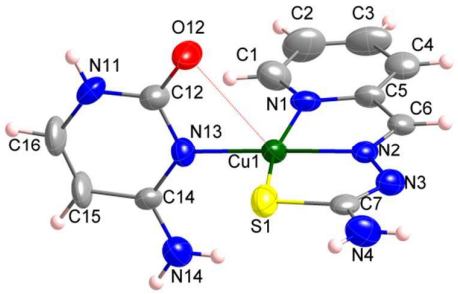

Fig. 4. Crystal structure of $[CuL(Hcyt)]^+$ entities in ***4***. Thermal ellipsoids are drawn at the 50% probability level.

A plethora of noncovalent interactions are responsible for the stabilization of the structures described here, such as π–π stacking, anion–π or hydrogen bonds (see text, Figs. S2–S4 and Tables S5–S7 in Supporting Information). Taking into account the different planar moieties, three possible types of π–π stacking could be considered, namely thiosemicarbazone···thiosemicarbazone, nucleobase···nucleobase and thiosemicarbazone···nucleobase, (Scheme 3a to 3c). In our case, although the most prominent π–π stacking interactions are those involving thiosemicarbazones for all of the studied structures (Scheme 3a), thiosemicarbazone···nucleobase interactions (compound ***2***) and nucleobase···nucleobase (compounds ***3*** and ***4***) are also observed (see Table S9). On the other side, hydrogen bonds are set up between thiosemicarbazones and nucleobase N atoms.

Spectroscopic and magnetic characterization. The usual IR bands for the pyridine-2-carbaldehyde thiosemicarbazonatocopper(II) entities,[33] together with those of the corresponding nucleobases and that attributed to perchlorate, nitrate and phosphate groups are observed (see Experimental Section, description in Supporting Information and Figs. S5–S10). Distortion in the perchlorate ions becomes υ_1 and υ_2 into IR active modes, similar to those described for a cytosinecopper(II) derivative[31] containing free perchlorate anions involved in strong hydrogen bonds. The very strong band at 1632 cm^{-1} for ***4*** can be assigned to the ν(CO) upon (C=O···Cu) coordination[17] and shifts to higher energy (1664 cm^{-1}) in free Hcyt, which supports the pseudocoordination between the Cu(II) ion and the oxygen carbonyl atoms.[34] However, the band associated to ν(CO) in ***3*** appears at 1683 cm^{-1}, without variation respect to the free 9-Mgua. The EPR signals and average *g* values are similar to those reported in the Literature for other nucleobase- and nucleotidecopper(II) derivatives (Fig. S11 and Experimental Section).[35] A more detailed discussion is given in Supporting Information.

View Article Online
DOI: 10.1039/C6DT02907H

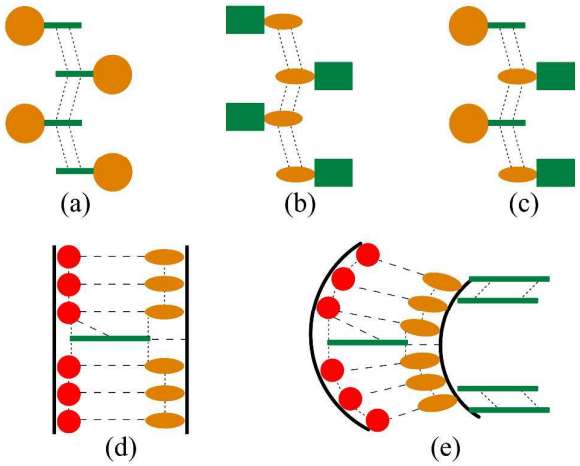

Scheme 3. Drawing of the π–π stacking (dotted lines) between thiosemicarbazonecopper(II) entities (green) (a), biomolecules aromatic rings (orange) (b) and between thiosemicarbazones and biomolecules (c). Proposed interaction mechanism between RNA and $[CuL(OH_2)]^+$, at low (d) and high (e) concentration of $[CuL(OH_2)]^+$. Red, orange and green blocks stand for uracil, Hade and $[CuL(OH_2)]^+$, respectively, dotted lines stand for π–π stacking and dashed lines for H-bonding.

The thermal evolution of χ_m and $\chi_m T$ for ***1*** (Fig. 5) is characteristic of antiferromagnetic behaviour, but all our attempts to fit it to analytical expressions for dinuclear or 1D Cu(II) systems were unsuccessful. The presence of interdinuclear interactions in compound ***1*** cannot be discarded. In this regard, we tried to evaluate the influence of intermolecular interactions by measuring the magnetic susceptibility of the monomer compound ***5*** (Fig. 6). The curve also denotes the presence of antiferromagnetic interactions and was fitted by Bleaney–Bowers equation [36] for dinuclear Cu(II) compounds derived from Heisenberg isotropic spin Hamiltonian $H = -2JS_1S_2$. The best least-square fitting is reached for $J/K = -2.3$ K and $g = 2.109$, which is very similar to that measured by EPR, $g = 2.085$.

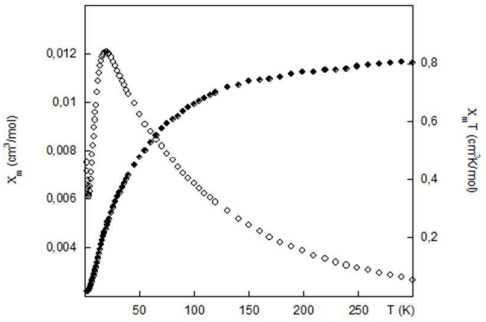

Fig. 5. Graphics of χ_m (◊◊◊), and $\chi_m T$ (♦♦♦) *versus* T for ***1***.

To explain the weak antiferromagnetic behaviour detected in ***5,*** two possible exchange pathways through noncovalent contacts can be proposed. On one hand, the already described π–π stacking, that involves chelating rings of different $[CuL(Hcyt)]^+$ entities with centroid···centroid distances in the 3.25–3.73 Å range but, even clearer, a separation between the copper and N3 nitrogen atom from a neighbour monomer of only 2.92 Å. Magnetic propagation through π–π stacking has been described for other Cu(II)-containing monomers[37] and dimers.[38] Other possible pathway for exchange coupling

View Article Online
DOI: 10.1039/C6DT02907H

would be the hydrogen bonding that relates the closest Cu1A and Cu1B centres in ***5***. The presence of even relatively intense magnetic coupling in hydrogen bonded Cu(II)-monomeric compounds has been discussed both in experimental[39] and theoretical studies.[40] Taking into account the presence of weak antiferromagnetic coupling in ***5*** despite the very short Cu···Cu distance in its structure, we suggest that the magnetic interactions in ***1***, clearly stronger than those in ***5***, are mainly intradinuclear in nature.

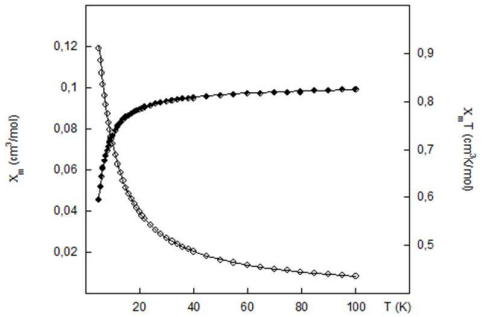

Fig. 6. χ_m (◊◊◊) and χ_mT (♦♦♦) *versus* T plots for ***5***. The corresponding fittings are represented by continuous lines.

Interaction of $[CuL]^+$ with RNA in aqueous solution.

In an earlier contribution,[17] we showed that $[CuL]^+$ interacts in aqueous solution with the nucleobases Hade, Hgua and Hcyt and their corresponding nucleotides dAMP, dGMP and dCMP, the affinity with the nucleobases being greater. For thymine and dTMP no interaction was observed. The equilibrium constant showed that methylation of the N9 guanine site considerably reduces the affinity with $[CuL]^+$. Thus, the apparent binding constant, $K_{app} = 6.3\times10^4$ M^{-1} for the CuL(9-Mgua) complex is two orders less than that measured for the CuL(gua) complex, $K_{app} = 5.4\times10^6$ M^{-1}. This result indicates that $[CuL]^+$ in solution mainly interacts with the N9 guanine site, but other types of interaction are also feasible.

The interaction of $[CuL]^+$ with $[poly(dA–dT)]_2$, $[poly(dG–dC)]_2$, and ctDNA has been probed in aqueous solution at pH 6.0, I = 0.1 M, and T = 25 °C, revealing that this metal complex acts as a groove binder with $[poly(dA–dT)]_2$ whereas it acts as a weak external binder with $[poly(dG–dC)]_2$ and ctDNA. By contrast, the $[CuL]^+$ binding to RNA still remains unexplored. In this section, we show that stacking interactions of the thiosemicarbazone···nucleobase and thiosemicarbazone··· thiosemicarbazone types are present also in solution in near physiological conditions. Moreover, hydrogen bond and electrostatic interactions also govern the formation of $[CuL]^+$ /RNA complex.

To gain some more insights into the possible interaction of the thiosemicarbazonecopper(II) dye with RNA, it is important to learn the binding ability of $[CuL]^+$ towards uracil. Uracil bears close similarity with thymine and in neither case coordination to $[CuL]^+$ has been observed. However, H bond between the H_2O ligands linked to $[CuL]^+$ and the oxygen of uracil in A–U base pairs is possible, as shown below.

The binding of $[CuL]^+$ to the synthetic RNA double helix, poly(rA)poly(rU) can be represented in terms of Eq. (1),

View Article Online
DOI: 10.1039/C6DT02907H

$$P + D \underset{}{\overset{K}{\rightleftharpoons}} PD \qquad (1)$$

where P and D stand for the poly(rA)□poly(rU) free binding sites and $[CuL]^+$, respectively, and PD stands for $[CuL]^+$/ poly(rA)□poly(rU) complex, C_D and C_P being the analytical P and D concentrations, respectively.

The thermal stability of the poly(rA)□poly(rU) double helix was studied by DSC in the absence and in the presence of different amounts of $[CuL]^+$. The melting temperature increased (ΔT_m = 28ºC) tending to a plateau at C_D/C_P = 0.1 (Fig. 7a), indicating that poly(rA)□poly(rU) becomes strongly stabilized for very low $[CuL]^+$ concentration; the pronounced increase in T_m can be consistent with an intercalated complex formed by one $[CuL]^+$ entity every ten RNA base-pairs, that is, $n' = 10$. By contrast, for the $[CuL]^+/[poly(dA–dT)]_2$ system, it turned out ΔT_m = 0.6ºC in the same concentration range;[17] thus, thermal stabilization of DNA by $[CuL]^+$ is less than for RNA, evincing the possibility of molecular recognition of duplex RNA over duplex DNA. As computational calculations will demonstrate (see below), intercalation and hydrogen bonds yield an interstrand-intercalated $[CuL]^+$ /RNA complex that can explain the strong stabilization of the RNA double helix by $[CuL]^+$.

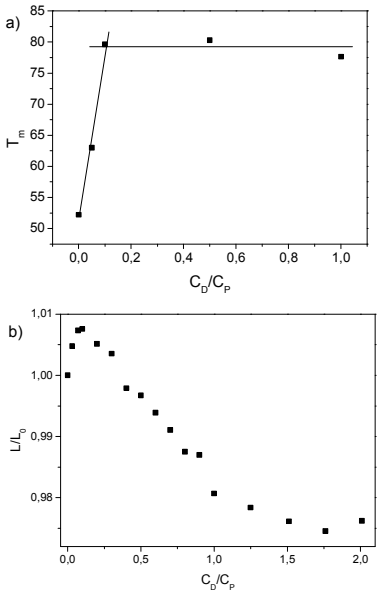

Fig. 7. a) DSC Melting temperature, T_m, versus C_D/C_P ratio. C_P = 0.5 mM; b) Variation of contour length with C_D/C_P ratio for the $[CuL]^+$/poly(rA)•poly(rU) system. C_P = 0.2 mM. I = 2.5 mM, pH = 6.0 and T = 25 ºC.

The DSC results are supported by viscosity measurements. The viscosity ratio η/η_0, where η_0 is the viscosity of the polymer alone and η is the viscosity of the dye/polynucleotide system, is related to the polynucleotide elongation by $L/L_0 = (\eta/\eta_0)^{1/3}$,[41] where L is the contour length of the dye/polynucleotide system and L_0 is that of the free polynucleotide. L/L_0 was plotted as a function of the C_D/C_P ratio. The evolution of the RNA contour length with the increase in relative viscosity (Fig. 7b), confirms the formation of an intercalated complex at low $[CuL]^+$ /RNA ratio, $C_D/C_P \sim 0.1$. By contrast, the diminution of viscosity for $C_D/C_P > 0.1$ indicates that a new complex is forming upon increase of the $[CuL]^+$ concentration. Figure S14 compares the viscosity data here described with those relative to different $[CuL]^+$ /DNA systems.[18] Unlike RNA, with DNA the L/L_0 ratio remained constant, indicating

View Article Online
DOI: 10.1039/C6DT02907H

that the type of binding strongly depends on the type of polynucleotide, RNA or DNA. The results attained with RNA for low C_D/C_P are consistent with intercalation up to $C_D/C_P = 0.1$, and with external or groove binding with DNA throughout the overall concentration range. Computational calculations bear out these conclusions and explain the main features of the intercalated $[CuL]^+$/ RNA complex.

The mode of interaction of $[CuL]^+$ with poly(rA)poly(rU) for the intercalative behaviour was optimized with two poly(rA)poly(rU) base-pairs. The resulting structures are shown in Fig. 8a and 8b. Before interaction, the average stacking distance between base pairs was 3.51 Å. When the $[CuL(OH_2)]^+$ complex (that formed when one aqua ligand from the solvent occupies the forth position in the square-planar polyhedron around the metal center) is inserted between A–U base pairs, stacking interactions in the intercalated system remain. As summarized in Table 1, the average distance between the upper A–U base-pair and $[CuL(OH_2)]^+$ is 3.51 Å, whereas it is 3.42 Å between the bottom A–U base-pair and $[CuL(OH_2)]^+$, the π–π stacking interaction of the latter being stronger compared to the upper base pairs. Moreover, the system is stabilized by a very strong H bond between the aqua ligand of $[CuL(OH_2)]^+$ and one oxygen of uracil, $O_{aqua}\cdots O_{uracil}$ 2.70 Å (Fig. 8b). Same calculations were performed for free poly(rG)poly(rC) and $[CuL]^+$/poly(rG)poly(rC), obtaining a preference for intercalation over external binding. The resulting structures are depicted in Fig. 8C and 8D. Intercalation of $[CuL]^+$ into G-C sequences promotes a higher base pair separation (4.77 Å and 3.88 Å to upper and bottom base pair respectively) than that obtained for poly(rA)poly(rU), which causes that hydrogen interaction between $[CuL]^+$ and the base pairs no longer exists. Thus, the stability of intercalated $[CuL]^+$ in RNA (A-U) sequences is 40.67 kcal/mol more stable than in RNA (G-C) sequences. In order to compare $[CuL]^+$/RNA with $[CuL]^+$/DNA behavior similar calculations were performed for DNA poly(dG)poly(dC) but no convergence of the calculation was possible, thus confirming the experimental results where no interaction of $[CuL]^+$ with poly(dG)poly(dC) was observed[18] and the RNA recognition by $[CuL]^+$.

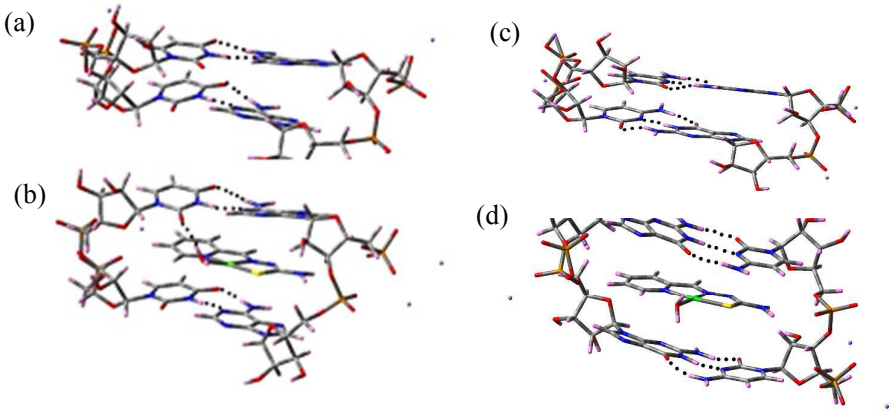

Fig. 8. QM/MM optimized structures of (a) free poly(rA)•poly(rU), (b) $[CuL]^+$/poly(rA)•poly(rU), (c) free poly(rG)•poly(rC) and (d) $[CuL]^+$/poly(rG)•poly(rC)in water. Colouring: C (grey), H (pink), O (red), S (yellow), P (brown) and Cu (green).

An analysis of the resulting RNA conformations from the optimizations for both free and bound RNA confirms the intercalative mode of binding of the dye. The optimized structures for free and bound RNA clearly visualize the elongation of the base-pair distance caused by intercalation. The small RNA base-pairs studied are considerably flexible and the possible orientations of the A-U and G-C units do

View Article Online
DOI: 10.1039/C6DT02907H

not provide essential information about the system when x and y axes are analyzed. Nonetheless, the Rise and Twist parameters for z axis (interpreted as the distance between base pairs and the unwinding angle respectively) can be obtained; these are the two main parameters considered for intercalation. The Rise parameter changed from 2.95 Å for free poly(rA)poly(rU) to 6.2 Å when $[CuL]^+$ intercalates, and from 3.29 Å to 7.07 Å in the case of poly(rG)poly(rC). Thus, the 100% increase in RNA elongation concurs with the first branch observed in viscosity measurements (Fig. 7b). The high value obtained for the Rise parameter could explain the huge *n*' value calculated above (*n*'= 10) since strong distortion of a site implies exclusion of the adjacent sites. The long distance between the A–U base pairs due to intercalation entails a non-cooperative behaviour. Moreover, insertion of the dye in the hydrophobic environment of the polynucleotides involves unwinding followed by decrease in helicity. Therefore, the twist parameter evolves from 34.56° to 23.37°, showing 11.19° unwinding angle (Table 1) which is greater than the obtained after $[CuL]^+$ intercalation in (2.29°) poly(rG)poly(rC). Scheme 3d schematically represents the complex intercalated into RNA.

Table 1. Average distances, Rise and Twist values for free poly(rA)•poly(rU) and $[CuL]^+$/poly(rA)•poly(rU) systems, obtained from QM/MM optimizations.

System	Upper $[CuL]^+$/AU, GC distance, (Å)	Lower $[CuL]^+$/AU, GC distance, (Å)	Rise, (Å)	Twist, (º)
Free poly(rA)•poly(rU)	-	-	2.95	34.56
$[CuL]^+$/poly(rA)•poly(rU)	3.52	3.42	6.20	23.37
Free poly(rG)•poly(rC)	-	-	3.29	30.30
$[CuL]^+$/poly(rG)•poly(rC)	4.77	3.88	7.07	28.01

Spectrophotometric titrations of the $[CuL]^+$/poly(rA)poly(rU) system were carried out at 0.0025, 0.10 and 1.0 M ionic strength. The spectral changes recorded upon addition of increasing amounts of poly(rA)poly(rU) to a $[CuL]^+$ solution, up to saturation, were smaller as the ionic strength rose; Fig. 9a shows the spectra recorded for I = 0.0025 M. The binding isotherm (Fig. 9a, inset) reveals the formation of the $[CuL]^+$/poly(rA)poly(rU) complex (PD), according to Eq. 1. The equilibrium constant, K, can be calculated by Eq. (2),

$$\frac{C_D}{\Delta A} = \frac{1}{\Delta\varepsilon} + \frac{1}{\Delta\varepsilon K}\cdot\frac{1}{[P]} \qquad (2)$$

where the polymer free-site concentration is expressed as $[P] = C_P \times f(r)$, with $f(r) = [1 - nr]^n/[1 - (n - 1)r]^{(1-n)}$. Evaluation of the concentration of polynucleotide free binding sites in equilibrium, [P], requires knowledge of the site size, *n*, defined as the number of base-pairs occupied by a bound drug molecule under saturation conditions.[42] The intersection of the two branches of the spectrophotometric titration curves yields the *n* value at the X axis,[43] (Fig. 9a, inset). The value obtained, *n* = 2, indicates that, for the $[CuL]^+$/poly(rA)•poly(rU) saturated complex, one could expect one $[CuL]^+$ molecule every two A–U base-pairs, whereas for low C_D/C_P ratio it turned out *n*'= 10 in the intercalated complex (see above). That is, an intercalated-external-aggregate complex can be formed, in which five $[CuL]^+$ units exist every ten base-pairs (roughly, a full helix turn); therefore, one $[CuL]^+$ molecule is

View Article Online
DOI: 10.1039/C6DT02907H

intercalated and the other four molecules (possibly forming two dimers, see Scheme 3e) are externally bound.

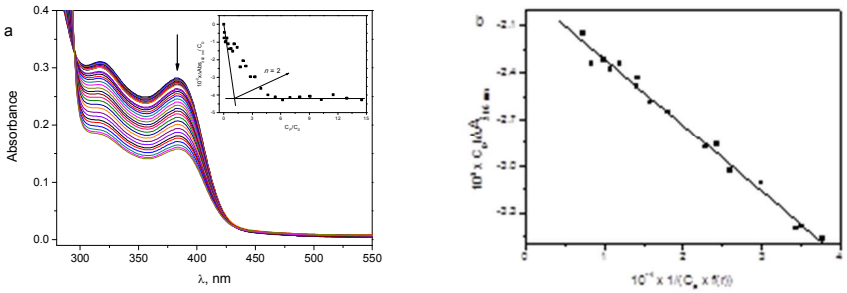

Fig. 9. a) Absorption spectra of the $[CuL]^+$/poly(rA)•(rU) system and binding isotherm at λ = 382 nm (Inset). b) Linear fitting of equation 2 to the spectrophotometric data. C_D = 26 μM, C_P/C_D = 0 − 15, I = 2.5 mM, pH = 6 .0 and T = 25 ºC.

Literature on the solid-state structure confirms the tendency of the $[CuL]^+$ entities to forming polynuclear compounds (mainly dinuclear) through covalent bond, in which thioamide S (S-bridged systems) and ancillary X ligand (X_bridged systems) play an important role.[3,25,44,45] In particular, it is noticeable the crystal structure of $[\{CuL(OH_2)\}_2]^{2+}$ S-bridged dimers recently reported,[45] very close to those proposed here. Except for Hcyt, our structural studies with nucleobases support this tendency. In addition, a wide range of noncovalent interactions (mainly hydrogen bond and π–π stacking) support the formation of aggregates in the crystals of these ternary species, presumably due to their planarity and the presence of heteroatoms. Even though previous studies have described the collapse of the polynuclear entities in solution to give monomeric $[CuL(OH_2)_n]^+$ entities,[46] recently published works have also detected $[Cu_2L_3]^+$ species at neutral pH.[47] All these features provide structural support for the aggregate formation in the vicinity of RNA.

Thus, the externally bound molecules forming dimers are responsible for the shortening of RNA, the observed diminution of relative viscosity for $C_D/C_P > 0.1$ evincing the interaction of the thiosemicarbazonecopper(II) on the RNA surface (Fig. 7b). These results are in full agreement with the DSC melting experiments for $C_D/C_P > 0.1$, the $[CuL]^+$ dimers located outside the helix having no influence on T_m (Fig. 7a). This finding has led us to assume that the intercalated thiosemicarbazone complex favours an ordered architecture along the RNA surface. Scheme 3e outlines the bifunctional external-intercalated complex. The π–π stacking interactions between thiosemicarbazonecopper(II) units are similar to those shown in Scheme 3a, whereas the intercalated complex is formed by interaction between thiosemicarbazones and biomolecules, such as those indicated in Scheme 3c. In other words, the π–π stacking interactions are present both in the solid state and in solution, both in the absence and in the presence of RNA.

The binding constants calculated by means of eqn 2 (Fig. 9b), differ by almost an order of magnitude, from $(4.5 \pm 0.7) \times 10^4$ M^{-1} at I = 2.5 mM to $(6.5 \pm 0.7) \times 10^3$ M^{-1} at I = 0.1 M and are too low to be evaluated precisely at I = 1 M. This behaviour indicates that electrostatic interactions are also present in the formation of $[CuL]^+$/poly(rA)•poly(rU) complex. The interaction between the positive charge of the copper dimers and the phosphate groups also play a key role that makes the formation of an external complex easier.

View Article Online
DOI: 10.1039/C6DT02907H

Is there any structural support for the way in which the thiosemicarbazonecopper(II) aggregates are linked to RNA? Unfortunately, we have not succeed in crystallizing nucleotide derivatives and, as the N9 (Hade) atom is linked to the ribose sugar in nucleotides, covalent bonds observed for our compounds in solid state between Cu(II) and N9 (Hade) are absent in RNA. On the other hand, previous chemical and crystallographic studies have described compounds in which phosphate groups bind to $[CuL]^+$ fragments such as $[(CuL)_4P_2O_7]\cdot nH_2O$ [48] and $[\{Cu(HL)(H_2PO_4)\}_2](H_2PO_4)_2\cdot 2H_3PO_4\cdot 2H_2O$.[49] Likewise, careful study of the structures of 18 mononucleotidecopper(II) derivatives extracted from the Cambridge Structural Database (CSD),[50] reveals no appreciable influence of anion-π interactions through the phosphate moieties, but rather coordination of the metal ions to at least two different phosphate oxygen atoms and setting of strong H bonds involving the phosphate groups. However, the coordination ability of the mononucleotide phosphate groups for the $[CuL]^+$ entities in water seems to be relatively low, perhaps due to the terdentate nature of HL against the maximum bidentate behaviour of the ancillary ligands that constitute the mononucleotidecopper(II) complexes in the Database. By contrast, although solution studies should reveal interaction between $[CuL]^+$ entities and H_2dTMP or H_2UMP, actually no reaction has been observed. This fact does not exclude the presence of electrostatic interactions with the phosphate scaffold in the RNA macromolecule, which seem to dominate in the reaction of $[CuL]^+$ and $[CuL']^+$ derivatives with synthetic DNA $[poly(dG\text{-}dC)]_2$ and ct-DNA.[18] Therefore, the tendency of these thiosemicarbazonecopper(II) systems to forming H bonds could lead to noncovalent links with the phosphate groups in the macromolecular nucleotides.

Lastly, the Circular Dichroism (CD) spectra recorded at different C_D/C_P ratios show significant structural changes in the RNA double helix (Fig. 10). The molar ellipticity at λ = 300 nm increases with the concentrations ratio and the positive band of RNA suffers a 3 nm bathochromic shift, characteristic of intercalating agents.[51]

The set of results gathered reveals that formation of the $[CuL]^+$/poly(rA)poly(rU) complex is governed by different types of interactions. That is, with the exception of covalent links, under physiological conditions the same noncovalent interactions observed in the solid state are at work in $[CuL]^+$/RNA solutions. This behaviour differs from that observed with DNA. Groove binding occurs with $[poly(dA–dT)]_2$, whereas it acts as an external binder with $[poly(dG–dC)]_2$ and/or ct-DNA. $[CuL]^+$ intercalates into RNA only at low concentration, $C_D/C_P \leq 0.1$; that is, the concentration and type of polynucleotide, DNA or RNA, plays a key role in the biological interaction of $[CuL]^+$. A similar behaviour, groove binding in DNA A-T tracts and intercalation in RNA, has been observed with cationic drugs such as Hoechst 33258, berenil or DAPI, which are considered to display molecular recognition since the binding may lie within duplex areas adjacent to bulges or loops, where such opening is available for threading intercalation to occur.[21 21] Thiosemicarbazonecopper(II) flat entities open a new avenue for medical applications blocking biological events related to RNA.

View Article Online
DOI: 10.1039/C6DT02907H

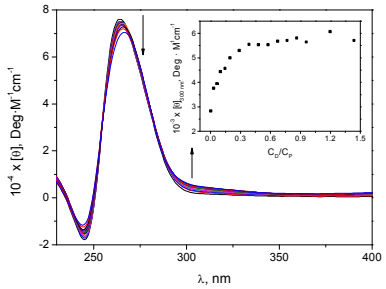

Fig. 10. CD spectra for the $[CuL]^+$/poly(rA)•poly(rU) system and molar ellipticity at λ = 300 nm (inset).

Conclusions

Ternary compounds containing thiosemicarbazonecopper(II) $[CuL]^+$ entities linked to Hade, Hcyt and 9-Mgua have been synthesized and characterized in solid state. For the first time, we describe here adenine- and guanine-containing thiosemicarbazone compounds and their structures. As far as we are aware, *[(CuL)$_2$(Hade)][{CuL}{CuL(OClO$_3$)}(ade)](ClO$_4$)$_2$·2H$_2$O* (***2***) represents the first compound whose crystal structure contains, clearly differentiated, both neutral and anionic adenines, *and [{CuL(9-Mgua)}$_2$(OH$_2$)](ClO$_4$)$_2$* (***3***) the unique one containing first-transition metal ions linked to S-donor ligands and guanine. Under the experimental conditions employed, no reaction is observed with thymine and uracil. A plethora of noncovalent interactions stabilize the lattice in the crystal structures reported, in particular hydrogen bonds, π–π stacking and anion–π interactions. The spectroscopic and magnetic properties also show the influence of these noncovalent linkages, which can illustrate the behaviour observed in the reaction of $[CuL]^+$ complexes with RNA in near physiological conditions. An intercalated, very stable $[CuL]^+$/RNA complex is formed for low Cu-thiosemicarbazone concentrations, $[CuL]^+ < 0.1$ [RNA]. Computational studies reveal that this intercalative behaviour could be due to both the strong π–π stacking and hydrogen bond interactions. The latter involves the aqua ligand of $[CuL(OH_2)]^+$ species and the oxygen atom of a carbonyl group from uracil. In fact, the presence of two carbonyl groups in uracil, keeping one of them available for establishing hydrogen bonding with non-nucleobase fragments, could also influence, at least in part, the great tendency for the intercalation into RNA at low concentrations. This very relevant interaction indicates that $[CuL]^+$ could play an important role in medical applications by blocking biological events related to RNA. When the $[CuL]^+$/RNA ratio is raised, an external complex is formed from the intercalated. The different behaviour of $[CuL]^+$ against DNA and RNA suggests a marked role of the macromolecule conformation in the type and intensity of the interactions.

Experimental Section

Chemicals. Copper(II) nitrate trihydrate, copper(II) perchlorate hexahydrate, sodium hydroxide, thiosemicarbazide, pyridine-2-carbaldehyde, cytosine, thymine, guanine, 9-methylguanine, adenine, adenosine-5′-monophosphate monohydrate and adenosine-5′-triphosphate disodium salt hydrate were

View Article Online
DOI: 10.1039/C6DT02907H

purchased from commercial sources and used as received. Published methods were used to synthesize HL, [52] HL′, [53] CuL(NO_3) [54] and [{CuL′(ONO_2)}$_2$]. [55] Aqueous solutions of uracil, 9-Mgua and poly(rA)□poly(rU) were prepared by dissolving the lyophilized sodium salts in doubly distilled water from a Millipore Q apparatus (APS, Los Angeles, California). Aqueous solutions of CuL(NO_3) 1 mM were used as source of $[CuL]^+$ entities. Stock solutions were prepared in [$NaClO_4$] = 0.1 or 1 M, using 2.5 mM sodium cacodylate [$Na(CH_3)_2AsO_2$] as a buffer to maintain the pH at 6.0. The poly(rA)□poly(rU) concentration as base pairs molarity was evaluated spectrophotometrically at λ = 260 nm using ε = 14900 $M^{-1}cm^{-1}$. The nucleobases and polynucleotide concentration is denoted as C_P and, in the case of the poly(rA)□poly(rU), is expressed in molarity of base-pairs, M_{BP}. The stock solutions of nucleobases and polynucleotide were kept in the dark at 4 ºC whereas the aqueous solutions of the dyes were freshly prepared. **CAUTION:** Perchlorate salts and their respective metal complexes can be explosive and use of only small amounts of reactants is strongly recommended.

Synthesis of *ternary thiosemicarbazone-nucleobase-copper(II) compounds.* ***[{CuL}{CuL(OH_2)}(ade)](ClO_4) (1) and [(CuL)$_2$(Hade)][{CuL}{CuL($OClO_3$)}(ade)](ClO_4)$_2$·2H_2O (2).*** An amount of Hade (0.5 mmol, 0.068 g) was dissolved in water (30 ml) and its pH adjusted to 7.4 with NaOH 1 M. An aqueous solution (35 ml) containing $Cu(ClO_4)_2·6H_2O$ (0.5 mmol, 0.185 g) and HL (0.5 mmol, 0.090 g) was stirred for 30 min and, afterwards, poured into the Hade one. The pH of the resulting mixture was raised to 7.4 by adding NaOH and the suspension was stirred for 2 h. A dark green solid of ***1*** was filtered off (yield 87 %, 0.161 g). Anal. found: C, 30.58; H, 2.68; N, 24.72; S, 8.60. Calc. for $C_{19}H_{20}ClCu_2N_{13}O_5S_2$ (737.13 g/mol): C, 30.96; H, 2.73; N, 24.70; S, 8.70. IR bands (cm^{-1}, KBr pellet): 3418 s, 3336 s, 3165 m, 1644 s, 1605 s, 1559 w, 1484 m, 1451 vs, 1439 w, 1400 w, 1383 w, 1357 w, 1325 m, 1297 m, 1266 w, 1226 m, 1171 s, 1151 s–$\upsilon_3(ClO_4^-)$, 1111 s–$\upsilon_3(ClO_4^-)$, 1090 s–$\upsilon_3(ClO_4^-)$, 973 m–$\upsilon_2(ClO_4^-)$, 905 m, 880 m, 772 m, 742 m, 625 m, 520 w, 451 m–$\upsilon_1(ClO_4)$, 412 m. Q-band EPR signals at RT: g_1 = 2.175, g_2 = 2.052 and g_3 = 2.043. Single crystals of compounds ***1*** and ***2*** suitable for X-ray diffraction measurements were obtained as follows: solid HL (0.5 mmol, 0.090 g) was slowly added to $Cu(ClO_4)_2·6H_2O$ (0.5 mmol, 0.185 g) in water (30 ml). On the other hand, solid Hade (0.5 mmol, 0.068 g) and 20 ml MeOH were poured into an aqueous solution (20 ml) of $Cu(ClO_4)_2·6H_2O$ (0.5 mmol, 0.185 g) at pH 5−6 by addition of NaOH. Both solutions were stirred separately for 1 h and, afterwards, that containing methanol was dropwise added onto the other and the mixture stirred for 2 h. Slow evaporation in air of the resulting solution yielded crystals of ***1*** and ***2***.

[(CuL)$_2$(Hade)][{CuL}{CuL($OClO_3$)}(ade)](ClO_4)$_2$·2H_2O (2). Several experimental procedures were carried out to develop a rational method to attain ***2***. As a result, different solids were obtained showing elemental analysis and spectroscopic properties in good agreement with the presence of different hydration degrees per unit formula, ranging from 2 (compound ***2***) to 10 water molecules. The fully characterized and reproducible phase was performed as follows. Hade (1.0 mmol, 0.136 g) and HL (1.0 mmol, 0.180 g) were dissolved in a refluxing water:methanol (1:1) mixture at 50 ºC for 2 h. Afterwards, $Cu(ClO_4)_2·6H_2O$ (1.0 mmol, 0.371 g) in 10 ml of methanol was poured into the ligands solution and kept with stirring at room temperature for 1 h. The solution was filtered off to eliminate insoluble impurities and was left for slow evaporation in air during several days. Dark blue-greenish crystals were isolated (yield 53 %, 0.214 g). Anal. found: C, 28.74; H, 2.85; N, 22.91; S, 7.89. Calc. for $C_{38}H_{41}Cl_3Cu_4N_{26}O_{14}S_4$ (1574.72 g/mol): C, 28.98; H, 2.62; N, 23.13; S, 8.15. IR bands (cm^{-1}, KBr pellet): 3430 w, 3312 s, 3118 s, 1650 vs, 1603 vs, 1572 w, 1490 s, 1447 vs, 1406 w, 1314 w, 1227 m, 1227 m, 1170 m, 1157 s–$\upsilon_3(ClO_4^-)$, 1111 s–$\upsilon_3(ClO_4^-)$, 1061 vs–$\upsilon_3(ClO_4^-)$, 917 m, 876 m, 774 m, 723 m, 618 m–$\upsilon_4(ClO_4^-)$, 514 m, 450 w, 416 m. FAB^+ mass spectrometry (m/z): 241.88 $[CuL]^+$, 376.89

View Article Online
DOI: 10.1039/C6DT02907H

$[CuL(Hade)]^+$, 619.74 $[(CuL)_2(Hade)]^+$. X-band EPR signal of polycrystalline powder at RT: g = 2.079.

{CuL(9-Mgua)}$_2$(OH$_2$)](ClO$_4$)$_2$ ***(3)***. Solid $Cu(ClO_4)_2{\cdot}6H_2O$ (0.3 mmol, 0.112 g) and HL (0.6 mmol, 0.118 g) were dissolved in 20 ml of a water:MeOH 1:1 solvent mixture. The pH of this solution was raised from 2.5 to 6.2 dropping 1 M aqueous NaOH. In a different baker, a solution of $Cu(ClO_4)_2{\cdot}6H_2O$ (0.3 mmol, 0.112 g) in 10 ml water was added to a suspension of 9-Mgua (0.6 mmol, 0.112 g) in 20 ml of water:MeOH 1:1. These solutions were stirred separately for 30 min. Afterwards, the former was poured drop by drop into the latter. Next, the acidity was adjusted at pH 6.5 by adding NaOH 1 M and a green solid was filtered off (0.158 g). After 6 weeks, slow evaporation of mother liquors at room temperature yielded few single crystals of ***3*** suitable for X-ray diffraction measurements.

A new way to attain powdery samples was optimized. $Cu(ClO_4)_2{\cdot}6H_2O$ (0.5 mmol, 0.185 g) was dissolved in 7 ml of distilled water. Solid 9-Mgua (0.5 mmol, 0.0832 g) was added and NaOH 1 M was dropped into to pH 6, whereas the reaction was stirred for 1 h. Then, solid HL (0.5 mmol, 0.090 g) was added, the pH was adjusted to 6 and the mixture was stirred for 3 h. A brown-greenish precipitate was filtered off and washed with water and acetone (yield 65 %, 0.335 g). Anal. found: C, 30.19; H, 3.30; N, 24.16; S, 6.15. Calc. for $C_{26}H_{30}Cl_2Cu_2N_{18}O_{11}S_2$ (1032.78 g/mol): C, 30.24; H, 2.93; N, 24.41; S, 6.21. IR bands (cm^{-1}, KBr pellet): 3464 s, 3397 s, 3278 w, 3160 s, 1683 vs, 1653 vs, 1626 vs, 1594 vs, 1557 s, 1496 m, 1480 m, 1427 vs, 1412 s, 1374 w, 1328 m, 1290 w, 1228 m, 1167 s, 1153 s (υ_3-ClO_4^-), 1112 vs (υ_3-ClO_4^-), 1068 vs (υ_3-ClO_4^-), 934 w, 914 w (υ_1-ClO_4^-), 890 w, 877 m, 777 m, 728 m, 692 w, 666 w, 624 s (υ_4-ClO_4^-), 523 m, 478 m, 444 m, 413 m. FAB^+ mass spectrometry (m/z): 242.02 $[CuL]^+$, 407.03 $[CuL(9\text{-Mgua})]^+$, 648.00 $[(CuL)_2(9\text{-Mgua})]^+$. X-band EPR signal of polycrystalline powder at RT: $g_{\|}$ = 2.140 and $g_{\perp}$ = 2.042.

[CuL(Hcyt)](ClO$_4$)·2H$_2$O ***(4)***. Solid HL (0.5 mmol, 0.090 g) was added to a solution of $Cu(ClO_4)_2{\cdot}6H_2O$ (0.5 mmol, 0.185 g) in 30 ml of water. On the other hand, $Cu(ClO_4)_2{\cdot}6H_2O$ (0.5 mmol, 0.185 g) was dissolved in 20 ml of water, basified up to pH = 5-6 with diluted NaOH. Then, 20 ml MeOH were poured into the solution. Next, solid Hcyt (0.5 mmol, 0.063 g) was added to the last mixture. Both solutions were stirred for 1 h and filtered off. Afterwards, the solution with Hcyt was dripped over the solution with $[CuL]^+$ entities. The resulting dark green solution was stirred at room temperature for 2 h and it was kept at room temperature. After few days, slow evaporation of the mother liquors yielded dark green single crystals suitable for X-ray diffraction measurements. Anal. found: C, 27.09; H, 3.11; N, 19.98; S, 6.37. Calc. for $C_{11}H_{16}ClCuN_7O_7S$ (489.36 g/mol): C, 27.00; H, 3.30; N, 20.04; S, 6.55. IR bands (cm^{-1}, KBr pellet): 3430 s, 3318 s, 3113 m, 1682 s, 1632 vs, 1564 w, 1526 m, 1485 w, 1449 s, 1441 s, 1378 w, 1322 m, 1298 w, 1274 w, 1231 m, 1172 w, 1151 m (υ_3-ClO_4^-), 1109 s (υ_3-ClO_4^-), 1087 vs (υ_3-ClO_4^-), 911 m (υ_1-ClO_4^-), 880 m, 792 w, 776 m, 765 m, 741 m, 730 m, 629 s (υ_4-ClO_4^-), 516 m. FAB^+ mass spectrometry (m/z): 242.09 $[CuL]^+$, 353.07 $[CuL(Hcyt)]^+$. Q-band EPR signals at RT: g_1 = 2.168, g_2 = 2.048 and g_3 = 2.033.

[CuL(Hcyt)](ClO$_4$) ***(5)***. The structure and characterization of this complex has been published previously by our group.[17] Here, we present a rational synthetic procedure for its achievement and EPR characterization not reported so far. A solution of $Cu(ClO_4)_2{\cdot}6H_2O$ (0.5 mmol, 0.185 g) and HL (0.5 mmol, 0.090 g) in 20 ml water was stirred for 30 min. Next, a solution of Hcyt (0.5 mmol, 0.063 g) in 10 ml of same solvent was poured into it and the pH was adjusted to 4 by adding NaOH 0.1 M.

View Article Online
DOI: 10.1039/C6DT02907H

The mixture was stirred for 24 h. Afterwards, a green solid was filtered off, washed with water and dried over vacuum (25 %, 0.056 g). Q-band EPR signals at RT: $g_1 = 2.169$, $g_2 = 2.047$ and $g_3 = 2.037$.

$(CuL)_2(cyt)(ClO_4)(H_2O)_2$ ***(6).*** A solution of $Cu(ClO_4)_2{\cdot}6H_2O$ (0.5 mmol, 0.185 g) and HL (0.5 mmol, 0.090 g) in 20 ml of water was stirred for 30 min. Next, a solution of Hcyt (0.5 mmol, 0.063 g) in 10 ml of the same solvent was poured, the pH was adjusted to 7.4 and it was stirred for 2 h. Finally, a green solid was isolated (24 %, 0.044 g). Anal. found: C, 29.27; H, 3.18; N, 20.94; S, 8.99. Calc. for $C_{18}H_{22}ClCu_2N_{11}O_7S_2$ (731.11 g/mol): C, 29.57; H, 3.03; N, 21.07; S, 8.77. IR bands (cm^{-1}, KBr pellet): 3410 m, 3317 m, 3184 m, 3085 m, 1640 s, 1602 s, 1567 m, 1533 m, 1487 m, 1448 w, 1436 vs, 1379 w, 1322 m, 1293 m, 1269 w, 1231 m, 1170 s, 1149 s (υ_3-ClO_4^-), 1109 s (υ_3-ClO_4^-), 1087 s (υ_3-ClO_4^-), 880 m, 776 m, 737 m, 627 m (υ_4-ClO_4^-), 558 m, 456 w (υ_3-ClO_4^-). FAB^+ mass spectrometry (m/z): 242.05 $[CuL]^+$, 353.05 $[CuL(Hcyt)]^+$, 483.97 $[Cu_2L_2]^+$, 594.00 $[(CuL)_2(cyt)]^+$. Q-band EPR signals at RT: $g_1 = 2.173$, $g_2 = 2.053$ and $g_3 = 2.037$.

$(CuL)_2(cyt)(NO_3)(H_2O)_2$ (7). The compound $CuL(NO_3)$ (1 mmol, 0.305 g) was dissolved in 100 ml water at 50 ºC and Hcyt (1 mmol, 0.112 g) was added as a solid. The mixture was stirred for 2 h at room temperature and then (pH = 4.5), it was filtered off. A dark green solid (54 %, 0.187 g) was washed with water and acetone and dried over vacuum. Anal. found: C, 31.50; H, 3.19; N, 24.62; S, 8.92. Calc. for $C_{18}H_{22}Cu_2N_{12}O_6S_2$ (693.67 g/mol): C, 31.17; H, 3.20; N, 24.23; S, 9.24. IR bands (cm^{-1}, KBr pellet): 3404 m, 3320 m, 3107 m, 1645 vs, 1605 s, 1593 s, 1570 s, 1532 s, 1486 s, 1445 vs, 1384 s (υ_3-NO_3^-), 1352 s, 1317 m, 1294 s, 1262 m, 1228 s, 1169 vs, 1153 m, 917 w, 881 m, 823 w (υ_2-NO_3^-), 800 w, 789 w, 776 m, 737 m, 684 w, 627 m, 600 w, 524 w, 496 w, 457 w, 418 w. Q-band EPR signals at RT: $g_{\|} = 2.052$ and $g_{\perp} = 2.110$.

$CuL'(Hcyt)(NO_3)(H_2O)$ ***(8)***. The preparation method for this compound was the same as the previous one but, in this case, the reagent was $[\{CuL'(ONO_2)\}_2]$ (0.5 mmol, 0.319 g) instead of $(CuL)(NO_3)$. After 2 h of vigorous stirring the solution pH was 7.2, and 15 days later, a dark green solid was filtered off, washed with water and acetone and dried over vacuum (12 %, 0.053 g). Anal. found: C, 32.58; H, 3.88; N, 24.65; S, 7.35. Calc. for $C_{12}H_{16}CuN_8O_5S$ (447.92 g/mol): C, 32.18; H, 3.60; N, 25.02; S, 7.16. IR bands (cm^{-1}, KBr pellet): 3450 w, 3279 m, 3082 m, 1683 m, 1651 w, 1630 vs, 1589 w, 1569 w, 1529 s, 1478 w, 1447 w, 1371 w, 1354 vs (υ_3-NO_3^-), 1312 m, 1289 s, 1225 s, 1179 w, 1154 w, 1115 m, 1099 w, 1035 m, 907 m (υ_2-NO_3^-), 783 w, 771 w, 741 w, 686 w, 650 w, 612 w, 560 w, 543 w, 518 w, 492 vw, 444 vw, 414 w. FAB^+ mass spectrometry (m/z): 256.05 $[CuL']^+$. Q-band EPR signals at RT: $g_1 = 2.172$, $g_2 = 2.050$ and $g_3 = 2.035$.

$(CuL)_2(ade)(NO_3)(H_2O)_5$ ***(9)***. The compound $CuL(NO_3)$ (0.5 mmol, 0.152 g) was dissolved in 50 ml of water at 50 ºC. Once dissolved, a solution of Hade (0.5 mmol, 0.068 g) in water (30 ml) was added and the resulting mixture was stirred for 2 h at room temperature, while pH is adjusted at pH 7.4 by addition of NaOH. A month later, dark green crystals were collected, but they decomposed immediately after removing the solvent. Several attempts to stabilize crystals of this compound were unsuccessful. Anal. found: C, 29.95; H, 3.65; N, 25.24; S, 7.95. Calc. for $C_{19}H_{28}Cu_2N_{14}O_8S_2$ (771.70 g/mol): C, 29.57; H, 3.66; N, 25.41; S, 8.31. IR bands (cm^{-1}, KBr pellet): 3402 s,b, 3305 w,sh, 3159 m, 1637 s, 1602 s, 1558 w, 1491 m, 1446 s, 1384 m (υ_3-NO_3^-), 1321 w, 1296 w, 1226 m, 1170 m, 1151 m, 1107 m, 908 m, 879 w, 827 w (υ_2-NO_3^-), 772 w, 725 w, 658 w, 623 w, 517 w, 414 w. FAB^+ mass spectrometry (m/z): 242.13 $[CuL]^+$, 377.08 $[CuL(Hade)]^+$, 484.03 $[Cu_2L_2]^+$, 618.10 $[(CuL)_2(ade)]^+$.

View Article Online
DOI: 10.1039/C6DT02907H

Synthesis of ternary thiosemicarbazone-nucleotide-copper(II) compounds. *$(CuL)_2(AMP)(H_2O)_8$ **(10)***. H_2AMP (0.2 mmol, 0.073 g) was dissolved in water (10 ml) and pH fixed at 6.0 by addition of an aqueous NaOH solution. Solid HL (0.4 mmol, 0.072 g) was slowly added to a solution of $Cu(ClO_4)_2 \cdot 6H_2O$ (0.4 mmol, 0.148 g) in water (10 ml), and the green solution was stirred for 30 min and, afterwards, filtered over the nucleotide solution. The mixture was allowed to react for 1 h and the pH set to 6.0 with NaOH. A dark green solid is collected, washed with water and acetone and dried over vacuum (53 %, 0.127 g). Anal. found: C, 29.57; H, 4.16; N, 18.46; S, 6.68. Calc. for $C_{24}H_{42}Cu_2N_{13}O_{15}PS_2$ (974.86 g/mol): C, 29.57; H, 4.34; N, 18.68; S, 6.58. IR bands (cm^{-1}, KBr pellet): 3437 s, 3278 m, 3128 s, 1649 m, 1630 s, 1601 s, 1558 w, 1482 s, 1450 s, 1437 s, 1380 w, 1318 w, 1292 w, 1229 m, 1170 s, 1107 s (υ_3-PO_4^{3-}), 1087 s (υ_3-PO_4^{3-}), 976 m, 911 m, 880 d, 783 m, 731 w, 696 w, 625 m, 520 w (υ_4-PO_4^{3-}), 471 w, 420 w. Q-band EPR signals at RT: $g_1 = 2.188$, $g_2 = 2.067$ and $g_3 = 2.041$.

*$(CuL')_2(AMP)(H_2O)_8$ **(11)***. The method was basically the same as that previously described, using HL' (0.4 mmol, 0.078 g) instead of HL. Dark green solid, (51 %, 0.127 g). Anal. found: C, 31.01; H, 4.58; N, 18.29; S, 6.00. Calc. for $C_{26}H_{46}Cu_2N_{13}O_{15}PS_2$ (1002.92 g/mol): C, 31.14; H, 4.62; N, 18.16; S, 6.39. IR bands (cm^{-1}, KBr pellet): 3394 s,b, 3337 w,sh, 3218 s, 1636 s, 1595 m, 1574 m, 1531 s, 1497 m, 1464 s, 1393 s, 1355 m, 1307 m, 1244 m, 1174 s,1125 s (υ_3-PO_4^{3-}), 1075 s (υ_3-PO_4^{3-}), 979 s, 886 w, 776 w, 724 w, 624 w, 520 w (υ_4-PO_4^{3-}), 416 w. FAB^+ mass spectrometry (m/z): 256.07 $[Cu(L')]^+$. Q-band EPR signals at RT: $g_1 = 2.183$, $g_2 = 2.066$ and $g_3 = 2.048$.

*$(CuL)_3(H_2ATP)(ClO_4)(H_2O)_8$ **(12)***. $Cu(ClO_4)_2 \cdot 6H_2O$ (0.3 mmol, 0.111 g) was dissolved in water (20 ml) and solid HL (0.3 mmol, 0.054 g) was added. After 30 min, the mixture was filtered over a $Na_2H_2ATP \cdot nH_2O$ solution (0.3 mmol, 0.165 g) in water (30 ml). The resulting solution was basified to pH 7.4 by addition of diluted NaOH. The reaction was kept for 2 h, being the pH restored to 7.4. No precipitation was observed and the green solution was allowed to rest for slow evaporation. One month later, a dark green solid appeared, (44 %, 0.064 g). Anal. found: C, 25.42; H, 3.50; N, 16.11; S, 6.52. Calc. for $C_{31}H_{51}ClCu_3N_{17}O_{25}P_3S_3$ (1473.92 g/mol): C, 25.21; H, 3.48; N, 16.12; S, 6.37. IR bands (cm^{-1}, KBr pellet): 3407 s, 3298 w,sh, 3148 s, 1640 s, 1605 s, 1559 w, 1487 m, 1450 s, 1437 s, 1380 m, 1322 w, 1296 m, 1229 s, 1171 s, 1156 w,sh (υ_3-ClO_4^-)/(υ_3-PO_4^{3-}), 1091 s (υ_3-ClO_4^-)/(υ_3-PO_4^{3-}), 908 m, 878 w, 824 w, 773 w, 725 w, 627 w, 557 w, 521 w (υ_4-PO_4^{3-}), 416 w. Q-band EPR signals at RT: $g_1 = 2.170$, $g_2 = 2.082$ and $g_3 = 2.058$.

Physical measurements. The pH measurements were performed using a CRISON micro pH 2002 pH-meter fitted out with a combined glass electrode with a 3 M KCl solution as a liquid junction. Microanalyses were performed with a LECO CHNS-932 analyzer. FAB^+ mass spectrometry data were obtained on a Micromass AutoSpec. Thermal analysis measurements were performed in a Netzsch STA 449C and in a TA SDT 2960 instruments. Crucibles containing 20 mg samples were heated at 10 ºC/min under dry air atmosphere. IR spectra were obtained with samples prepared as KBr pellets in the 4000-400 cm^{-1} region on a Nicolett Impact 410 FTIR and a JASCO FT-IR 4200 spectrophotometer, the latter equipped with a Single Reflection ATR PRO ONE device. The intensity of reported IR bands are defined as vs = very strong, s = strong, m = medium and w = weak, while b stands for broad band. Room temperature X-band EPR spectra of powdered samples were recorded on a Bruker EMX spectrometer, equipped with a Bruker ER 036TM NMR-teslameter and an Agilent 53150A microwave frequency counter to fit the magnetic field and the frequency inside the cavity. Q-band measurements were carried out by a Bruker ESP300 spectrometer equipped with a Bruker BNM 200 gaussmeter and

View Article Online
DOI: 10.1039/C6DT02907H

a Hewlett-Packard 5352B microwave frequency counter to fit the magnetic field and the frequency inside the cavity. The simulation of the EPR spectra was performed using the SimFonia program.[56]

The spectrophotometric titrations were performed on a Hewlett-Packard 8453A (Agilent Technologies, Palo Alto, CA) photodiode array spectrophotometer with a Peltier temperature control system. Titrations were carried out by adding increasing amounts of uracil or RNA (P) into the cell containing the $[CuL]^+$ solution (D). The sample was not illuminated during the equilibration period. Circular dichroism (CD) measurements were performed with a MOS-450 Biological spectrophotometer (Bio-Logic SAS, Claix, France) fitted out with 1.0 cm path-length cells. Titrations were carried out at 25ºC by adding increasing amounts of $[CuL]^+$ to the RNA solution. The thermal denaturation behaviour was studied by DSC measurements, using a Nano DSC Instrument (TA, Waters LLC, New Castle, USA). To avoid bubbles formation upon heating, the reference and the sample solutions were previously degassed in a degassing station (TA, Waters LLC, New Castle, USA). The samples were scanned at 3 atm pressure from 20 to 90 °C at 1 °C·min^{-1} scan rate. Viscosity measurements were performed using a Micro-Ubbelohde viscometer (Schott, Mainz, Germany) immersed in a water bath at 25 ºC. The flow time was measured with a digital stopwatch. Sample viscosities were evaluated as the mean value of at least three replicated measurements. The viscosity data were analysed using $\eta/\eta_0 = (t - t_0)/(t_{RNA} - t_0)$, where t_0 and t_{RNA} are the solvent and polynucleotide solution flow times, respectively, whereas t is the flow time of the dye and poly(rA)·poly(rU) mixture. The viscosity readings were reported as $L/L_0 = (\eta/\eta_0)^{1/3}$ versus C_D/C_P ratio,[41] where η and η_0 stand for the polynucleotide viscosity in the presence and in the absence of dye, respectively.

Crystallographic structure determination. Crystal data collections were carried out on a Stoe IPDS I single-crystal diffractometer using monochromated MoKα radiation (λ = 0.71073 Å). Absorption corrections, when needed, were made using the Guassian integration. Direct methods (SIR97)[57] were employed to solve the structures and then refined using the SHELXL-2013 computer program[58] within WINGX.[59] The non-H atoms were refined anisotropically, using weighted full-matrix least-squares on F^2. The H atoms (excluding those of the water molecules) were included in calculated positions and refined as riding atoms with default SHELXL parameters. Selected crystallographic and refinement details for the four crystal structures are shown in Table 2. A more complete set of experimental and resolution parameters is given in Table S1. CCDC 1400120-1400123 contain the supplementary crystallographic data for **1**–**4**. These data can be obtained free of charge via http://www.ccdc.cam.ac.uk/conts/retrieving.html, or from the Cambridge Crystallographic Data Centre, 12 Union Road, Cambridge CB2 1EZ, UK; fax: (+44) 1223-336-033; or e-mail: deposit@ccdc.cam.ac.uk.

Computational details. In silico study was performed for the metal complex and RNA interaction with Gaussian 09[60] software. Prior to that study, structure optimization of the dye and a two base-pair poly(rA)poly(rU) and poly(rG)poly(rC) were carried out by running DFT studies, in water. For $[CuL(OH_2)]^+$ complex, ωB97X-D functional was employed, applying 6-31G basis with diffuse function (6-31G*) for light atoms (C, H O, N and S) and LANL2DZ for Cu, which has been employed by previous author in organometallic complexes.[61] This basis set consists of a Dunning/Hazinaga valence double-zeta basis, containing ECP (effective core potential) representations of core electrons for third row elements and beyond. Inclusion of ECP method replaces core electrons with an effective potential which, apart from taking into account relativistic effects, it considerably diminishes the calculation time, while maintaining the reliability.

View Article Online
DOI: 10.1039/C6DT02907H

Table 2. Crystallographic data for compounds ***1 - 4***.

	1	***2***	***3***	***4***
Empirical formula	$C_{19}H_{20}ClCu_2N_{13}O_5S_2$	$C_{38}H_{41}Cl_3Cu_4N_{26}O_{14}S_4$	$C_{26}H_{30}Cl_2Cu_2N_{18}O_{11}S_2$	$C_{11}H_{16}ClCuN_7O_7S$
Formula weight	737.13	1574.72	1032.78	489.36
Temperature (K)	293(2)	293(2)	293(2)	293(2)
Wavelength (Å)	0.71073	0.71073	0.71073	0.71073
Crystal system	Monoclinic	Monoclinic	Monoclinic	Triclinic
Space group	$P2_1/n$	$P2_1/a$	I2/a	$P\bar{1}$
A (Å)	9.120(2)	15.564(5)	17.661(10)	7.164(2)
B (Å)	21.317(4)	22.845(18)	9.779(3)	11.561(7)
C (Å)	13.736(3)	17.255(10)	22.809(8)	12.416(7)
α (°)	90	90	90	98.38(6)
β (°)	94.41(3)	97.41(6)	103.96(6)	104.31(4)
γ (°)	90	90	90	99.69(6)
Volume ($Å^3$)	2662.5(9)	6084(6)	3823(3)	963.1(8)
Z	4	4	4	2
Density (calc.) (Mg/m^3)	1.839	1.719	1.794	1.687
Absorption coefficient (mm^{-1})	1.916	1.731	1.445	1.431
R indices [$I > 2\sigma(I)$]	R_1 = 0.0503	R_1 = 0.0688	R_1 = 0.0470	R_1 = 0.0571
	wR_2 = 0.0646	wR_2 = 0.0980	wR_2 = 0.1148	wR_2 = 0.1219

Two free base-pair poly(rA)□poly(rU) and $[CuL]^+$/2poly(rA)□poly(rU) calculations were run with Quantum Mechanics/Molecular mechanics method, QM/MM. In QM/MM calculations the accuracy of Quantun Mechanics is combined with the speed of Molecular Mechanics. For this work, the QM part of the system was applied to uracil, Hade and $[CuL(OH_2)]^+$ moieties, treated with the same method applied for free organometallic complex described above. The MM part of this calculation consists of the RNA backbone, and was studied with AMBER94[62] force field, using electronic embedding for setting the charges of the RNA. Sodium atoms were added to the MM part in order to maintain the polynucleotide electroneutrality.

View Article Online
DOI: 10.1039/C6DT02907H

DNA parameters were analyzed with X3DNA[63] software, as the number of base pairs is short, dye/DNA interaction was analyzed in terms of one translational (Rise) and one angular base-pair step parameters (Twist).[64] Rise parameter gives a value for adjacent base-pairs separation on the long axis (z axis) of polynucleotides and Twist shows the helix unwinding.

Acknowledgements

We thank Dr. J.J. Delgado, Dr. Pilar Castroviejo, Marta Mansilla (SCAI, Universidad de Burgos, Spain) for the elemental analysis and mass spectra and Elena Rita Alonso (University of Valladolid, Spain) for lending us her computational cluster. This work was supported by Obra Social "la Caixa" (OSLC-2012-007), Ministerio de Economía y Competitividad and FEDER funds (CTQ2013-48937-C2-1-P, CTQ2015-70371-REDT, MAT2012-34740 and CTQ2014-58812-C2-2-R), Junta de Castilla y León (BU237U13), the Basque Government (IT-779-13), Gerencia Regional de Salud, Consejería de Sanidad, Junta de Castilla y León (GRS 1023/A/14 and GR172) and Projects. Universidad de Burgos and Caja de Burgos, Spain, are also gratefully acknowledged. R. G.–G. wishes to thank to the Junta de Castilla y León for his Doctoral Fellowship.

References

1 R. W. Brockman, J. R. Thomson, M. J. Bell and H. E. Skipper, *Cancer. Res.*, **1956**, *16*, 167.

2 S. Padhyé and G. B. Kauffman, *Coord. Chem. Rev.*, **1985**, *63*, 127.

3 J. García-Tojal, R. Gil-García, P. Gómez-Saiz and M. Ugalde, *Curr. Inorg. Chem.*, **2011**, *1*, 189.

4 R. C. DeConti, B. R. Toftness, K. C. Agrawal, R. Tomchick, J. A. R. Mead, J. R. Bertino, A. C. Sartorelli and W. A. Creasey, *Cancer Res.*, **1972**, *32*, 1455.

5 R. A. Finch, M.-C. Liu, A. H. Cory, J. G. Cory and A. C. Sartorelli, *Advan. Enzyme Regul.*, **1999**, *39*, 3. L. Feun, M. Modiano, K. Lee, J. Mao, A. Marini, N. Savaraj, P. Plezia, B. Almassian, E. Colacino, J. Fischer and S. MacDonald, *Cancer Chemother. Pharmacol.*, **2002**, *50*, 223. J. Murren, M. Modiano, C. Clairmont, P. Lambert, N. Savaraj, T. Doyle and M. Sznol, *Clin. Cancer Res.*, **2003**, *9*, 4092. F. J. Giles, P. M. Fracasso, H. M. Kantarjian, J. E. Cortes, R. A. Brown, S. Verstovsek, Y. Alvarado, D. A. Thomas, S. Faderl, G. Garcia-Manero, L. P. Wright, T. Samson, A. Cahill, P. Lambert, M. Sznol, J. F. DiPersio and V. Gandhi, *Leuk. Res.*, **2003**, *27*, 1077. Y. Yen, K. Margolin, J. Doroshow, M. Gishman, B. Johnson, C. Clairmont, D. Sullivan, M. Sznol, *Cancer Chemother. Pharmacol.*, **2004**, *54*, 331. K. W. L. Yee, J. Cortes, A. Ferrajoli, G. Garcia-Manero, S. Verstovsek, W. Wierda, D. Thomas, S. Faderl, I. King, S. M. O'Brien, S. Jeha, M. Andreeff, A. Cahill, M. Sznol and F. J. Giles*, Leuk. Res.*, **2006**, *30*, 813. I. Gojo, M. L. Tidwell, J. Greer, N. Takebe, K. Seiter, M. F. Pochron, B. Johnson, M. Sznol and J. E. Karp, *Leuk. Res.*, **2007**, *31*, 1165.J. J. Knox, S. J. Hotte, C. Kollmannsberger, E. Winquist, B. Fisher and E. A. Eisenhauer, *Invest. New Drugs,* **2007**, *25*, 471. J. E. Karp, F. J. Giles, I. Gojo, L. Morris, J. Greer, B. Johnson, M. Thein, M. Sznol and J. Low, *Leuk. Res.*, **2008**, *32*, 71.

6 W. E. Antholine, P. Gunn and L. E. Hopwood, *Int. J. Rad. Oncol. Biol. Phys.,* **1981**, *7*, 49. F. A. French, E. J. Blanz, S. C. Shaddix and R. W. Brockman, *J. Med. Chem.*, **1974**, *17*, 172. J. García-

View Article Online
DOI: 10.1039/C6DT02907H

Tojal, A. García-Orad, A. Álvarez Díaz, J. L. Serra, M. K. Urtiaga, M. I. Arriortua and T. Rojo, *J. Inorg. Biochem.*, **2001**, *84*, 271. T. Varadinova, D. Kovala-Demertzis, M. Rupelieva, M. Demertzis and P. Genova, *Acta Virolog.*, **2001**, *45*, 87.

7 H. Beraldo and L. Tosi, *Inorg. Chim. Acta*, **1986**, *125*, 173. H. A. O. Hill, D. J. Page and N. J. Walton, *J. Electroanal. Chem.*, **1986**, *208*, 395. H. A. O. Hill, D. J. Page and N. J. Walton, *J. Electroanal. Chem.,* **1987**, *217*, 129.

8 D. B. Lovejoy, P. J. Jansson, U. T. Brunk, J. Wong, P. Ponka and D. R. Richardson, *Cancer Res.*, **2011**, *71*, 5871. K. L. Fung, A. K. Tepede, K. M. Pluchino, L. M. Pouliot, J. N. Pixley, M. D. Hall and M. M. Gottesman, *Mol. Pharmaceut.*, **2014**, *11*, 2692. A. Gaál, G. Orgován, Z. Polgári, A. Réti, V. C. Mihucz, S. Bösze, N. Szoboszlai and C. Streli, *J. Inorg. Biochem.*, **2014**, *130*, 52. K. Ishiguro, Z. P. Lin, P. G. Penketh, K. Shyam, R. Zhu, R. P. Baumann, Y.-L. Zhu, A. C. Sartorelli, T. J. Rutherford and E. S. Ratner, *Biochem. Pharmacol.,* **2014**, *91*, 312. M. A. Cater, H. B. Pearson, K. Wolyniec, P. Klaver, M. Bilandzic, B. M. Paterson, A. I. Bush, P. O. Humbert, S. La Fontaine, P. S. Donnelly and Y. Haupt, *ACS Chem. Biol.*, **2013**, *8*, 1621. F. Bisceglie, R. Alinovi, S. Pinelli, M. Goldoni, A. Buschini, S. Franzoni, A. Mutti, P. Tarasconi and G. Pelosi, *Metallomics*, **2013***, 5*, 1510. J. Shao, Z.-Y. Ma, A Li,. Y.-H. Liu, C.-Z. Xie, Z.-Y. Qiang and J.-Y. Xu, *J. Inorg. Biochem.*, **2014**, *136*, 13.

9 M. Belicchi Ferrari, F. Bisceglie, G. Gasparri Fava, G. Pelosi, P. Tarasconi, R. Albertini, S. Pinelli. *J. Inorg. Biochem.*, **2002**, *89*, 36–44 and references therein.

10 E. C. Moore, M. S. Zedeck, K. C. Agrawal, A. C. Sartorelli, *Biochemistry*, **1970**, *9*, 4492. L. Thelander and A. Gräslund, *J. Biol. Chem.,* **1983**, *258*, 4063.

11 W. C. Kaska, C. Carrano, J. Michalowski, J. Jackson and W. Levinson, *Bioinorg. Chem.*, **1978**, *3*, 245. M. Leigh, D. J. Raines, C. E. Castillo and A. K. Duhme-Klair, *ChemMedChem*, **2011**, *6*, 1107. F. Bacher, E. A. Enyedy, N. V. Nagy, A. Rockenbauer, G. M. Bognár, R. Trondl, M. S. Novak, E. Klapproth, T.Kiss and V. B. Arion, *Inorg. Chem.*, **2013**, *52*, 8895. F. Bisceglie, S. Pinelli, R. Alinovi, M. Goldoni, A. Mutti, A. Camerini, L. Piola, P. Tarasconi and G. Pelosi, *J. Inorg. Biochem*., **2014**, *140*, 111. K. Y. Djoko, B. M. Paterson, P. S. Donnelly, A. G. McEwan, *Metallomics*, **2014**, *6*, 854.

12 D. S. Raja, N. S. P. Bhuvanesh, K. Natarajan, *Eur. J. Med. Chem.*, **2011**, *46*, 4584. Z. C. Liu, B. D. Wang, Z. Y. Yang, Y. Li, D. D. Qin and T. R. Li, *Eur. J. Med. Chem*., **2009**, *44*, 4477. A. Q. Ali, S. G. Teoh, N. E. Eltayeb, M. B. K. Ahamed and A. M. S. A. Majid, *Polyhedron*, **2014**, *74*, 6.

13 A. M.Thomas, A. D. Naik, M. Nethaji and A. R. Chakravarty, *Inorg. Chim. Acta,* **2004**, *357*, 2315.

14 S. Arounaguiri, D. Easwaramoorthy, A. Ashokkumar, A. Dattagupta and G. M. Bashkar, *Proc. Indian Acad. Sci. Chem. Sci.*, **2000**, *112*, 219.

15 M. Baldini, M. Belicchi-Ferrari, F. Bisceglie, G. Pelosi, S. Pinelli and P. Tarasconi, *Inorg. Chem.*, **2003**, *42*, 2049.

View Article Online
DOI: 10.1039/C6DT02907H

16 M. Belicchi-Ferrari, F. Bisceglie, G. Pelosi, P. Tarasconi, *Polyhedron,* **2008**, *27*, 1361. S. Parveen, F. Arjmand , I. Ahmad, *J. Photochem. Photobiol. B,* **2014**, *130*, 170.

17 B. García, J. García-Tojal, R. Ruiz, R. Gil-García, S. Ibeas, B. Donnadieu and J. M. Leal, *J. Inorg. Biochem.*, **2008**, *102*, 1892.

18 R. Ruiz, B. García, J. García-Tojal, N. Busto, S. Ibeas, J. M. Leal, C. Martins, J. Gaspar, J. Borrás, R. Gil-García and M. González-Álvarez, *J. Biol. Inorg. Chem.*, **2010**, *15*, 515.

19 Y. Tor, *ChemBioChem* **2003**, 4, 998-1007. C. S. Chow and F. M. Bogdan, *Chem. Rev.* **1997**, *97*, 1489.

20 W. D. Wilson, L. Ratmeyer, M. Zhao, L. Strekowski and D. Boykin, *Biochemistry* **1993**, *32*, 4098.

21 B. Willis and D. P. Arya, *Bioorg. & Med. Chem.,* **2014**, *22*, 2327. N. Ranjan, S. Kumar, D. Watkins, D. Wang, D. H. Appella and D. P. Arya, *Bioorg. & Med. Chem. Lett.,* **2013**, *23*, 5689. S. Kumar, N. Ranjan, P. Kellish, C. Gong, D. Watkins and D. P. Arya, *Org. Biomol. Chem.,* **2016**, *14*, 2052. S. Nahar, N. Ranjan, A. Ray, D. P. Arya and S. Maiti, *Chem. Sci.,* **2015**, *6*, 5837.

22 F. Hueso-Urena, M. N. Moreno-Carretero and A. L. Penas-Chamorro, Inorg. *Chem. Commun.*, **1999**, *2*, 323. M. B. Ferrari, F. Bisceglie, G. Pelosi, P. Tarasconi, R. Albertini, A. Bonati, P. Lunghi and S. Pinelli, *J. Inorg. Biochem.,* **2001**, 83, 169.

23 P. Gómez-Saiz, R. Gil-García, M. A. Maestro, J. L. Pizarro, M. I. Arriortua, L. Lezama, T. Rojo and J. García-Tojal, *Eur. J. Inorg. Chem.*, **2005**, 3409.

24 R. Gil-García, R. Fraile, B. Donnadieu, G. Madariaga, V. Januskaitis, J. Rovira, L. González, J. Borrás, F. J. Arnáiz and J. García-Tojal, *New. J. Chem.*, **2013**, *37*, 3568.

25 P. Gómez-Saiz, J. García-Tojal, V. Díez-Gómez, R. Gil-García, J. L. Pizarro, M. I. Arriortua and T. Rojo, Inorg. *Chem. Commun.*, **2005**, *8*, 259. R. Gil-García, P. Gómez-Saiz, V. Díez-Gómez, B. Donnadieu, M. Insausti, L. Lezama and J. García-Tojal, *Polyhedron*, **2013**, *54*, 243.

26 PDF Release 2011; International Centre For Diffraction Data: Philadelphia (EE.UU.), **2011**.

27 R. Gil-García, R. Zichner, V. Díez-Gómez, B. Donnadieu, G. Madariaga, M. Insausti, L. Lezama, P. Vitoria, M. R. Pedrosa, J. García-Tojal, *Eur. J. Inorg. Chem*., **2010**, 4513.

28 D. Choquesillo-Lazarte, M. P. Brandi-Blanco, I. García-Santos, J. M. González-Pérez, A. Castiñeiras and J. Niclós-Gutiérrez, *Coord. Chem. Rev.*, **2008**, *252*, 1241. J. Cepeda, O. Castillo, J. P. García-Terán, A. Luque, S. Pérez-Yáñez and P. Román, *Eur. J. Inorg. Chem*., **2009**, 2344. S. Pérez-Yáñez, O. Castillo, J. Cepeda, J. P. García-Terán, A. Luque and P. Román, *Eur. J. Inorg. Chem.*, **2009**, 3889. D. K. Patel, A. Domínguez-Martín, M. D. P. Brandi-Blanco, D. Choquesillo-Lazarte, V. M. Nurch and J. Niclós-Gutiérrez, *Coord. Chem. Rev.*, **2012**, *256*, 193. S. Pérez-Yáñez, G. Beobide, O. Castillo, J. Cepeda, A. Luque and P. Román, *Cryst. Growth Des.*, **2012**, *12*, 3324. H. El Bakkali, A. Castiñeiras, I. García-Santos, J. M. González-Pérez and J. Niclós-Gutiérrez, *Cryst. Growth Des.*, **2014**, *14*, 249. J. Thomas-Gipson, G. Beobide, O. Castillo, M.

View Article Online
DOI: 10.1039/C6DT02907H

Fröba, F. Hoffmann, A. Luque, S. Pérez-Yáñez and P. Román, *Cryst. Growth Des.*, **2014**, *14*, 4019.

29 A. W. Addison, T. N. Rao, J. Reedijk and G. C. Verschoor, J. Chem. Soc., *Dalton Trans.*, **1984**, 1349.

30 A. García-Raso, J. J. Fiol, A. López-Zafra, A. Tasada, I. Mata, E. Espinosa and E. Molins, *Polyhedron*, **2006**, *25*, 2295. D. J. Szalda, L. G. Marzilli and T. J. Kistenmacher, *Inorg. Chem.*, **1975**, 14, 2076. M. Sundaralingam and J. A. Carrabine, *J. Mol. Biol.*, **1971**, *61*, 287. A. Panfil, A. Terrón, J. J. Fiol and M. Quiros, *Polyhedron*, **1994**, *13*, 2513.

31 M. Palaniandavar, I. Somasundaram, M. Lakshminarayanan and H. J. Manohar, *J. Chem. Soc., Dalton Trans.*, **1996**, 1333.

32 D. Voet and A. Rich, *Prog. Nucleic Acid Res. Mol. Biol.,* **1970**, *10*, 183. G. Cervantes, J. J. Fiol, A. Terrón, V. Moreno, J. R. Alabart, M. Aguilo, M. Gómez and X. Solans, *Inorg. Chem.*, **1990**, *29*, 5168.

33 J. García-Tojal, J. García-Jaca,; R. Cortés, T. Rojo, M. K. Urtiaga and M. I. Arriortua, *Inorg. Chim. Acta*, **1996**, *249*, 25. J. García-Tojal, L. Lezama, J. L. Pizarro, M. Insausti, M. I. Arriortua and T. Rojo, *Polyhedron*, **1999**, *18*, 3703.

34 H. Susi, J. S. Ard and J. M. Purcell, *Spectrochim. Acta, Part A*, **1973**, *29*, 725.

35 D. Choquesillo-Lazarte, A. Domínguez-Martín, A. Matilla-Hernández, C. S. Medina-Revilla, J. M. González-Pérez, A. Castiñeiras and J. Niclós-Gutiérrez, *Polyhedron*, **2010**, *29*, 170. J. L. García–Giménez, G. Alzuet, M. González–Álvarez, A. Castiñeiras, M. Liu–González and J. Borrás, *Inorg. Chem.,* **2007**, *46*, 71788. J. M. González–Pérez, C. Alarcón–Payer, A. Castiñeiras, T. Pivetta, L. Lezama, D. Choquesillo–Lazarte, G. Crisponi and J. Niclós-Gutiérrez, *Inorg. Chem.*, **2006**, *45*, 877. T. F. Mastropietro, D. Armentano, E. Grisolia, C. Zanchini, F. Lloret, M. Julve and G. De Munno, *Dalton Trans.,* **2008**, 514. S. Pérez–Yáñez, O. Castillo, J. Cepeda, J. P. García–Terán, A. Luque and P. Román, *Inorg. Chim. Acta*, **2011**, *365*, 211.

36 B. Bleany and K. D. Bowers, *Proc. R. Soc. London, Ser. A,* **1952**, 214, 451.

37 S. Das, G. P. Muthukumaragopal and S. Pal, *New J. Chem.*, **2003**, *27*, 1102.

38 C. Hou, J.–M. Shi, Y.–M. Sun, W. Shi, P. Cheng and L.–D. Liu, *Dalton Trans.*, **2008**, 5970.

39 W. Plass, A. Pohlmann and J. Rautengarten, *Angew. Chem. Int. Ed.*, **2001**, *40*, 4207. J. Tang, J. Sánchez Costa, A. Golobic, B. Kozlevcar, A. Rotertazzi, A. V. Vargiu, P. Gamez and J. Reedijk, *Inorg. Chem.*, **2009**, *48*, 5473.

40 C. Desplanches, E. Ruiz and S. Alvarez, *J. Chem. Soc., Chem. Commun.*, **2002**, 2614. C. Desplanches, E. Ruiz, A. Rodríguez–Fortea and S. Álvarez, *J. Am. Chem. Soc.*, **2002**, *124*, 5197.

41 G. Cohen and H. Eisenberg, *Biopolymers*, **1969**, *8*, 45.

42 J. D. McGhee and P. H.. von Hippel, *J. Mol. Biol.*, **1974**, *86*, 469.

View Article Online
DOI: 10.1039/C6DT02907H

43 N. Busto, B. García, J. M. Leal, J. F. Gaspar, C. Martins, A. Boggioni and F. Secco, *Phys. Chem. Chem. Phys.*, **2011**, 13, 19534.

44 J. García-Tojal, M. K. Urtiaga, R. Cortés, L. Lezama, T. Rojo and M. I. Arriortua, *J. Chem. Soc. Dalton Trans.*, **1994**, 2233. P. Gómez-Saiz, J. García-Tojal, A. Mendia, B. Donnadieu, L. Lezama, J. L. Pizarro, M. I. Arriortua and T. Rojo, *Eur. J. Inorg. Chem.*, **2003**, 518. P. Gómez-Saiz, J. García-Tojal, M. A. Maestro, J. Mahía, F. J. Arnáiz, L. Lezama and T. Rojo, *Eur. J. Inorg. Chem.*, **2003**, 2639.

45 R. Gil–García, P. Gómez-Saiz, V. Díez-Gómez, G. Madariaga, M. Insausti, L. Lezama, J. V. Cuevas and J. García–Tojal, *Polyhedron*, **2014**, *81*, 675.

46 L. A. Saryan, K. Mailer, C. Krishnamurti, W. Antholine and D. H. Petering, *Biochem. Pharmacol.*, **1981**, 30, 1595.

47 E. A. Enyedy, N. V. Nagy, É. Zsigó, C. R. Kowol, V. B. Arion, B. K. Keppler and T. Kiss, *Eur. J. Inorg. Chem.*, **2010**, 1717.

48 E. W. Ainscough, A. M. Brodie, J. D. Ranford, J. M. Waters and K. S. Murray, *Inorg. Chim. Acta,* **1992**, *197*, 107.

49 E. W. Ainscough, A. M. Brodie, J. D. Ranford and J. M. Waters, *J. Chem. Soc., Dalton Trans.,* **1997**, 1251.

50 Cambridge Crystallographic Data Centre, 12 Union Road, Cambridge CB2 1EZ, UK.

51 N. Busto, B. Garcia, J. M. Leal, F. Secco and M. Venturini, *Org. Biomol. Chem.,* **2012**, *10*, 2594.

52 F. E. Anderson, C. J. Duca and J. V. Scudi, *J. Am. Chem. Soc.*, **1951**, *73*, 4967.

53 D. X. West, D. L. Huffman, J. S. Saleda and A. E. Liberta, *Transition Met. Chem.*, **1991**, *16*, 565. D. X. West, G. A. Bain, R. J. Butcher, J. P. Jasinski, Y. Li, R. Y. Pozdiakiv, J. Valdés-Martínez, R. A. Toscano and S. Hernández-Ortega, *Polyhedron*, **1996**, *15*, 665.

54 A. G. Bingham, H. Bögge, A. Müller, E. W. Ainscough and A. M. Brodie, *J. Chem. Soc., Dalton Trans.*, **1987**, 493.

55 P. Gómez-Saiz, J. García-Tojal, M. A. Maestro, F. J. Arnáiz and T. Rojo, *Inorg. Chem.*, **2002**, *41*, 1345.

56 WINEPR SimFonia, version 1.25; Bruker Analytische Messtecnik GmβH: Rheinstetten, Germany 1996.

57 A. Altomare, M. C. Burla, M. Camalli, G. L. Cascarano, C. Giacovazzo, A. Guagliardi, A. G. G. Moliterni, G. Polidori and R. Spagna, *J. Appl. Crystallogr.*, **1999**, *32*, 115.

58 G. M. Sheldrick, *Acta Crystallogr*., **2008**, *A64*, 112.

59 L. J. Farrugia, WINGX; *J. Appl. Crystallogr.*, **2012**, *45*, 849.

View Article Online
DOI: 10.1039/C6DT02907H

60 M. J. Frisch, G. W. Trucks, H. B.Schlegel, G. E. Scuseria, M. A. Robb, J. R. Cheeseman, G. Scalmani, V. Barone, B. Mennucci, G. A. Petersson et al. Gaussian 09, Revision B.01. Gaussian 09, Revision B.01, Gaussian, Inc., Wallingford CT, 2009.

61 J. R. B.Gomes and J. A. N. F. Gomes, *Surf. Sci.*, **2001**, *471*, 59. G. Gahungu and J. Zhang. *Chem. Phys. Lett.*, **2005**, *410*, 302.

62 W. D. Cornell, P. Cieplak, C. I. Bayly, I. R. Gould, K. M. Merz, D. M. Ferguson, D. C. Spellmeyer, T. Fox, J. W. Caldwel and, P.A. Kollman. *J. Am. Chem. Soc.*, **1995**, *117*, 5179.

63 A. V Colasanti, X.-J. Lu and W. K. Olson. *J. Vis. Exp.*, **2013**, e4401.

64 X. Lu and W. K. Olson, *Nucleic Acids Res.*, **2003**, *31*, 5108.

View Article Online
DOI: 10.1039/C6DT02907H

Selectivity of a thiosemicarbazonatocopper(II) complex to duplex RNA. Relevant noncovalent interactions both in solid state and in solution

Rubén Gil–García,[a] María Ugalde,[a] Natalia Busto,[a] Héctor J. Lozano,[a] José M. Leal,[a] Begoña Pérez,[a] Gotzon Madariaga,[b] Maite Insausti,[c] Luis Lezama,[c] Roberto Sanz,[a] Lidia M. Gómez-Sainz[a] , Begoña García,*[a] and Javier García–Tojal*[a]

[a] Departamento de Química, Universidad de Burgos, 09001 Burgos, Spain
[b] Departamento de Física de la Materia Condensada, Universidad del País Vasco, Aptdo. 644, 48080 Bilbao, Spain
[c] Departamento de Química Inorgánica, Universidad del País Vasco, Aptdo. 644, 48080 Bilbao, Spain

Keywords: copper, nucleobase, nucleotide, RNA, thiosemicarbazone.

TOC Graphic

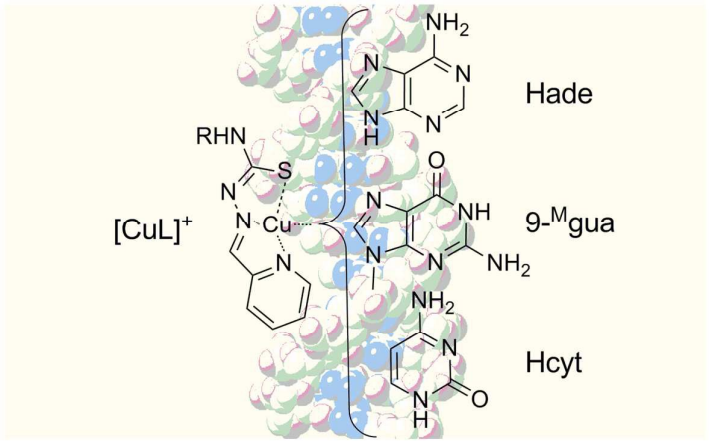

Intercalation of thiosemicarbazonecopper(II) $[CuL]^+$ species into RNA at low concentration affords an increase of melting temperature of 28 ºC, in contrast to the behaviour observed for DNA. The crystal structures of ternary $[CuL]^+$ / nucleobase compounds support the presence of strong non-covalent interactions, both in solid and solution, whose influence in the reactivity against DNA and RNA and biological relevance are discussed.